

Lista articolelor științifice publicate

A. Articole științifice publicate în reviste

1. Sergiu SOLCAN, Raul **ROZSOS**, BERE Paul, VLAD Nicolae, Grad DANIEL, Calin NEAMTU "Designing a car seat for electrical car", Acta Technica Napocensis Journal, Applied Mathematics, Mechanics & Engineering Series, Vol. 62, No. 4, 2019, ISSN: 1221-5872, pp: 617-622 (*ISI ESCI*);
2. Raul Silviu **ROZSOS**, Zsolt Levente BUNA, BODI Ștefan, Radu COMES, Vasile TOMPA "Design and development of a linear delta 3d printer" Acta Technica Napocensis Journal, Applied Mathematics, Mechanics & Engineering Series, Vol. 63, No. 2, 2020, ISSN: 1221-5872, pp: 185-190 (*ISI ESCI*);
3. Paul BERE, Raul **ROZSOS**, Cristian DUDESCU, Calin NEAMTU "Manufacturing method for bicycle saddle from carbon/epoxy composite materials" The Romanian Journal of Technical Sciences. Applied Mechanics. Vol. 64, No. 2, pp: 97-112;
4. Sergiu SOLCAN, Calin NEAMTU, Paul BERE, Rares GHINEA, Raul **ROZSOS**, Attila PAPP "Using composite materials for dashboard design of an electric car" Acta Technica Napocensis Journal, Applied Mathematics, Mechanics & Engineering Series, Vol. 62, No. 3, 2018, ISSN: 1221-5872, pp: 215-220 (*ISI ESCI*);
5. Sergiu SOLCAN, BODI Ștefan, Radu COMES, Raul Silviu **ROZSOS**, Calin NEAMTU, Cătălin COCEAN "Design and ergonomic analysis of car doors made from composite materials", Acta Technica Napocensis Journal, Applied Mathematics, Mechanics & Engineering Series, Vol. 64, No. 1, 2021, ISSN: 1221-5872, pp: 181-188 (*ISI ESCI*);
6. Rareș GHINEA, Vasile TOMPA, Zsolt BUNA, Raul **ROZSOS**, Daniela POPESCU, Ciprian FIREA, "Using image processing to authenticate artwork (II)", Acta Technica Napocensis Journal, Applied Mathematics, Mechanics & Engineering Series, Vol. 62, No. 4, 2019, ISSN: 1221-5872, pp: 601-606 (*ISI ESCI*);

Cluj-Napoca

22.06.2021

Drd. ing. Rozsos Raul Silviu



A handwritten signature in blue ink, appearing to read 'Rozsos'.



TECHNICAL UNIVERSITY OF CLUJ-NAPOCA

ACTA TECHNICA NAPOCENSIS

Series: Applied Mathematics, Mechanics, and Engineering
Vol. 62, Issue IV, November, 2019

DESIGNING A CAR SEAT FOR ELECTRICAL CAR

Sergiu SOLCAN, Raul ROZSOS, Paul BERE, Vlad NICOLAE,
Daniel GRAD, Calin NEAMTU

Abstract: The paper presents the design stages of an electric car seat using the Design Thinking methodology. The designed seat is made of composite materials dedicated to urban electric cars.

Key words: Design Thinking, electric car, car seats, composit materials.

1. INTRODUCTION

The paper presents the steps and how to develop and validate a seat for a small electric car from the L6e category. The development of this chair was made using a creative, innovative, iterative and cooperative Design Thinking algorithm.

DESIGN THINKING: A NON-LINEAR PROCESS

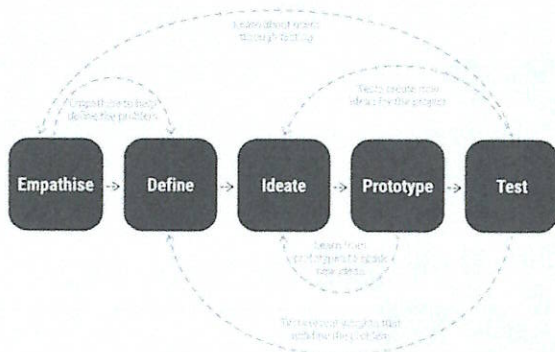


Fig. 1 Design Thinking [1]

The design team is an interdisciplinary one that includes designers, engineers, composite material specialists and ergonomics specialists.

2. EMPATIA - CAR SEATS DESIGN REVIEW

At this stage a careful and extensive research of the car seat design trends was carried out, the aim of the team was to identify the new trends in shape and design of materials and comfort

elements that are expected to be used on medium and long term by the main “actors” in the automotive sector. One of the trends identified in the market is the design and realization of monocoque chairs (Fig. 2).



Fig. 2 Monocoque car seats [2, 3]

These seats have a rigid resistance structure made of two or more components that assemble and over which assemble the parts that provide

Rozsos

the comfort of the sponge / foam the heating system and the material that confers the final shape and appearance of the seat.

A second interesting trend at the moment for a small electric car is the design of seats in the form of a banquet similar to those from the 80s (Fig. 3).



Fig. 3 Bench type seats [4, 5]

This type of seats is suitable for smaller spaces and offers a high level of comfort during short-term trips such as those in the urban area. In terms of materials, three different streams have been identified. The first uses the classic materials currently found on the market in the vast majority of automobiles: foam, textiles and natural or organic leather in various variants and combinations. The second identified trend uses composite materials based on glass fiber and / or carbon fiber to create chairs similar to those in the sports motor. The third trend is the use of new and unconventional materials such as various types of rubber and elastic materials that allow the removal of the design of the arcs and soft materials that provide the comfort of traditional seats Fig. 4.



Fig. 4 Kinetic Seat Lexus [6]

3. DEFINE - DESIGN SPECIFICATION

At this stage of development, the requirements for the seat that will be developed for the concept machine set out in Fig. 5.

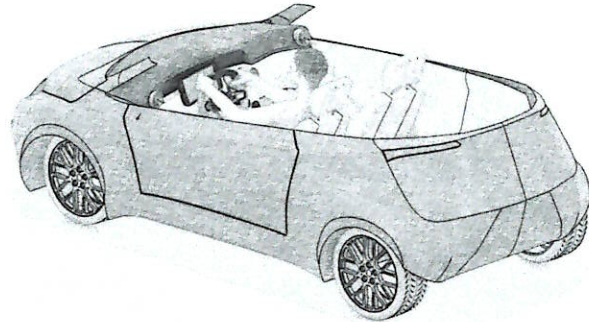


Fig. 5 URBIVEL Concept Car

The machine stitch will be made of carbon fiber composite material so that at this stage a constraint on the material and with it the manufacturing process is introduced. The design specifications are as follows:

- the seat should be monocoque
- assure the comfort needed for short and medium distances
- minimalist design similar to the sports seat seats
- ergonomic use
- possibilities for adjusting the horizontal position
- can be made with composite materials

Rozes

4. IDEATE – DESIGNING THE SEAT

This stage is an innovation and generates the solution to the problem. Through successive analyzes and improvements, a result that can be used in the prototyping stage is reached.

The first variant of the seat is shown in Fig. 6 and is similar to the seats in the sports motor. The shape of the seat allows the manufacture of composite materials, which will be lined with foam and textiles.



Fig. 6 Version 1

After the first model was followed, an analysis phase followed, using the Catia V5 / 6 to analyze the driving position of the driver. The position of the driver in the seat made of composite material is shown in Fig. 7 and is identical to the position in the classic seat, the seat line follows the natural body position.

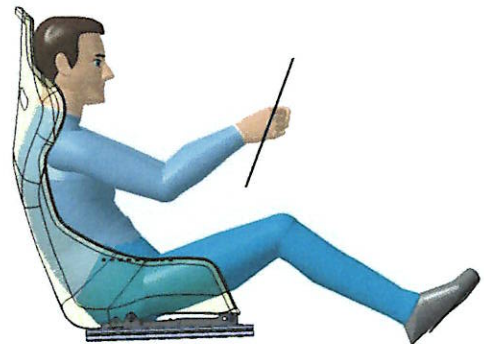
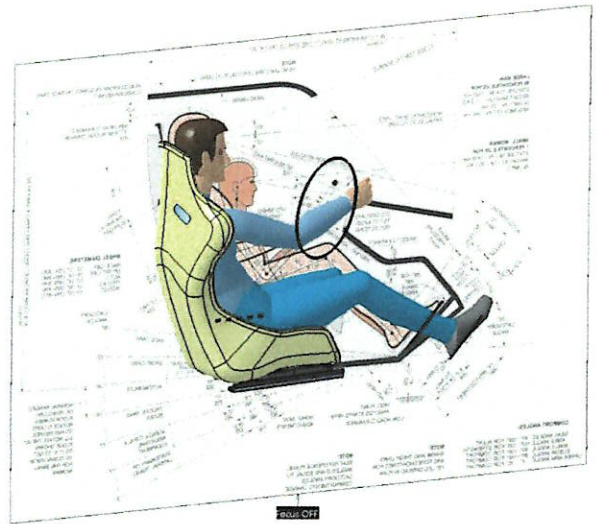


Fig. 7 Driver's position

After assembly of the seats in the body of the prototype (Fig. 8) one of the problems identified is a certain difficulty when the occupant is sitting in the seat because of the quite high edges. To remove this shortcoming, an asymmetric chair with one of the smallest sides is modeled to facilitate the positioning and lifting of the seat Fig. 9.



Fig. 8 Asymmetrical seats in the body of the prototype

Rozas

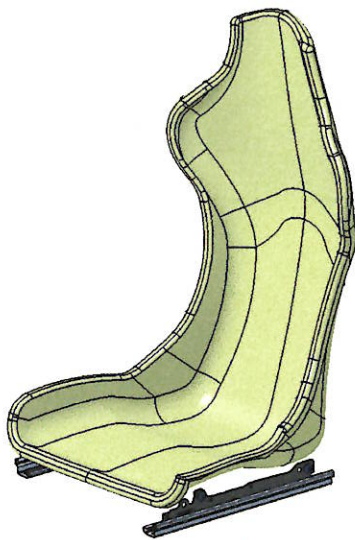


Fig. 9 Asymmetrical seat (Version 2)

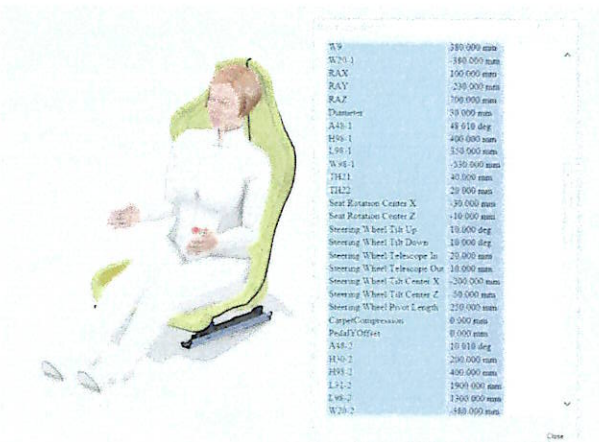


Fig. 10 Ergonomics analysis

To increase the comfort fence, design a one-piece chair that has a set of slots on the back and sides of the backrest to allow air circulation and increase the backrest elasticity, thus increasing comfort (Fig. 11). In this version of the seat, the surfaces were modeled in such a way that they could be made in a single mold. The advantage of such a chair is that it has a higher elasticity than the classic ones, is easy to maintain and can be used in combination with sponge cushions to increase the occupant's comfort. The low surface of the seat helps to accelerate acclimatization as there are areas (where there are cuts) where there

is no contact between the seat and the occupant's body.



Fig. 11 Car seat version 3

The seats designed so far offer only one degree of mobility, namely horizontal translation. The latest version of the seat offers a higher degree of comfort due to the folding back (Fig. 12).

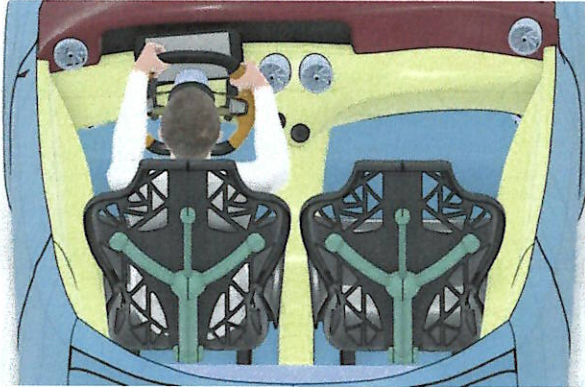


Fig. 12 Folding chair (Version 4)

The chairs designed so far offer only one degree of mobility, namely the horizontal translation. The last variant of the seat offers a higher degree of comfort due to the folding backrest (Fig. 12).

5. SEAT PROTOTYPE

For model prototyping (Fig. 13), two types of 3D printers were used: FDM (Leap Frog XL and

Dot Bot) and SLA (Form Lab2), and three 1:10 scales were printed (Fig. 14)



Fig. 13 Printed seat models

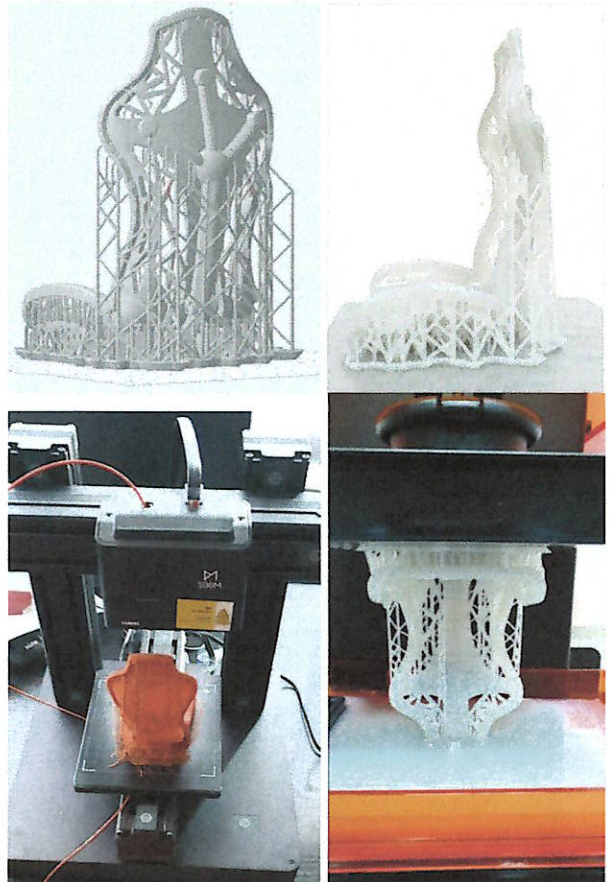


Fig. 14 Prototype printing

6. PROTOTYPE TESTING

Testing the prototype is to be done on the 1:1 scale model, at this stage studying the structure of the composite material and the orientation of the layers to provide the necessary elasticity to ensure the occupant's comfort without using foam or other soft materials.

Rozsa

7. CONCLUSIONS

The paper presents the steps of developing a car seat made of composite materials for an electric city car. The main innovation in this seat is the shape of the backrest and the sides of the seat, which features cutouts that give the seat an elasticity fence, allowing the soft padding of the seat and the better ventilation of the occupant. The chair is at the stage of designing the composite material and prototype manufacturing. The development of the chair was done using the Design Thinking method.

8. ACKNOWLEDGMENTS

This work was supported by the project "Advanced technologies for intelligent urban electric vehicles"- URBIVEL - Contract no.11/01.09.2016, project co-founded from the European Regional Development Fund through the Competitiveness Operational Program 2014-2020

9. REFERENCES

- [1]Soegaard, M., The Basics of User Experience Design. Interaction Design Foundation, ed. 2018:
- [2]Skoda-Auto, Vision E <http://www.skoda-auto.rs/company/visione>. 2019 [cited 2019 March].
- [3]FORD AUTOMOBILE, EVOS Interior Concept. 2019 [cited 2019 March]; Available from: <http://www.seriouswheels.com/2011/def/2011-Ford-Evos-Concept-Interior-1280x960.htm>.
- [4]BMW. BMW i3 Concept. 2018 [cited 2019 February]; Available from: <https://www.bimmertoday.de/2012/06/13/bmw-i3-concept-mit-seriennaherem-innenraum-in-london-prasentiert/>.
- [5]BUTTS, H.-M. Curbside Concepts: Honda Urban EV – Are Bench Seats Coming Back? 2017 [cited 2019 February]; Available from: <http://www.curbsideclassic.com/uncategorized/curbside-concepts-honda-urban-ev-are-bench-seats-coming-back/>.
- [6]Lexus. Lexus Kinetic Seat Concept World Premiere at the 2016 Paris Motor Show. 2016 [cited 2019 March]; Available from: <http://pressroom.lexus.com/releases/lexus-kinetic-seat-concept-premiere-2016-paris-motor-show.htm>

DESIGN SCAUN AUTO PENTRU MASINA ELECTRICA

Lucrarea prezinta etapele de proiectare a unui scaun pentru un automobil electric utilizând metodologia Design Thinking

Sergiu SOLCAN, Technical University of Cluj-Napoca, Design Engineering and Robotics, Bd. Muncii 103-105, Romania

Raul ROZSOS, Technical University of Cluj-Napoca, Design Engineering and Robotics, Bd. Muncii 103-105, Romania

Paul BERE, Technical University of Cluj-Napoca, Manufacturing Engineering, Bd. Muncii 103-105, Romania

Nicolae VLAD, Technical University of Cluj-Napoca, Automotive Engineering and Transportation, Bd. Muncii 103-105, Romania

Grad DANIEL, Eng., Belco-Avia SRL, Livezile Str. Cruci Nr. 423, Bistrita-Nasaud county, Romania

Calin NEAMTU, Technical University of Cluj-Napoca, Design Engineering and Robotics, Bd. Muncii 103-105, Romania.

Rozsos



TECHNICAL UNIVERSITY OF CLUJ-NAPOCA

ACTA TECHNICA NAPOCENSIS

Series: Applied Mathematics, Mechanics, and Engineering
Vol. 63, Issue II, June, 2020

DESIGN AND DEVELOPMENT OF A LINEAR DELTA 3D PRINTER

Raul-Silviu ROZSOS, Zsolt Levente BUNA, Stefan BODI, Radu COMES, Vasile TOMPA

Abstract: The paper presents the design process and the development of a linear Delta 3D printer. The most commonly used mechanical structure for Fused Deposition Molding (FDM) printers is based on the traditional parallel mechanism. This paper highlights the advantages of a Delta structure 3D printer in comparison with the Cartesian structures regarding various technical specifications such as accuracy, printing speed, layer thickness and the overall printer's size. AHP Instruments were used to identify the optimal design of the printer and a Pugh matrix was devised to obtain the best ranking of the possible 3D printing structures. The developed printer's accuracy has been compared with other market available Cartesian structure printers to highlight the accuracy paired with printing speed of the Delta 3D printer.

Key words: 3D printer, additive manufacturing, design, AHP

1. INTRODUCTION

Additive manufacturing (AM), commonly known as 3D printing, has been available commercially in the last 30 years. Still, the early prototypes were expensive. Thus, the widespread adoption of 3D printers has only happened after 2000 due to RepRap Project and other similar initiatives as well as the fact that the significant AM patents expired [1].

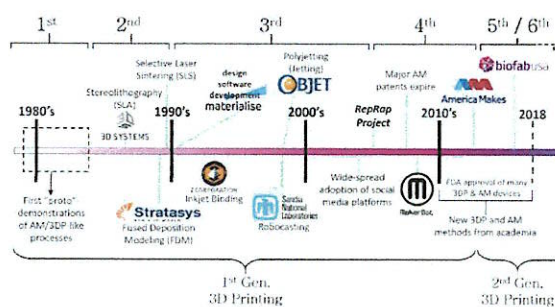


Fig. 1. The 3D printer development timeline in regards to the essential AM patents expire [1]

The first 3D printer patent was published in Google Patents in 1986 under the name of an Apparatus used to produce three-dimensional objects by stereo-lithography. The first 3D printer concept was developed by one of the co-founders of 3D Systems Company, one of the

leading companies in the 3D printers' market, which also extends towards 3D scanning and software development.

The global market for 3D printing market has rapidly evolved, and the attention has swapped from hobbyists towards various industries such as aerospace, automotive, electronics. The overall Additive Manufacturing market is projected to reach \$16 billion industry in 2020 and over \$40 billion in the following five years as it is presented in Statista [2].

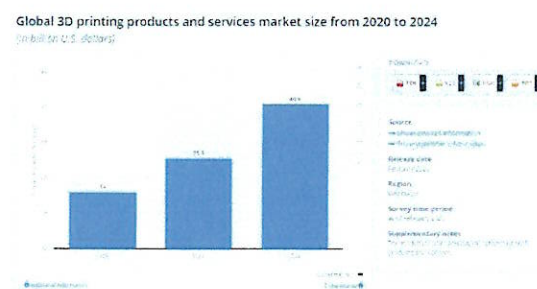


Fig. 2. 3D Printing products and service market size prediction 2020-2024 [2]

The increase market size of additive manufacturing has led some specialists to consider that this technology will be at the basis of the Fourth Industrial Revolution.

Rozsos

The most common 3D printing technologies on the market are the following:

- FDM – Fused Deposition Modeling
- SLA – Stereolithography
- DLP – Digital Light Processing
- SLS – Selective Laser Sintering
- SLM – Selective Laser Melting
- 3DP – Inkjet Tridimensional Printing
- LOM – Laminated Object Manufacturing
- PJP – PolyJet Printing

FDM type 3D printers are the most common, because the technology behind them is very accessible. These printers come in different shapes and sizes, with a variety of configurations, from the classic extruder (1-2 or more extruders, grouped or individual) to multi-tools (printing, laser engraving, CNC carving). The classification of 3D printers can be done in several ways, but the most common classification is related to their structure. Depending on their mechanical structure there are:

- Cartesian structure (Cartesian coordinates)
- Delta structure
- Polar structure (Polar coordinates)
- Scara structure

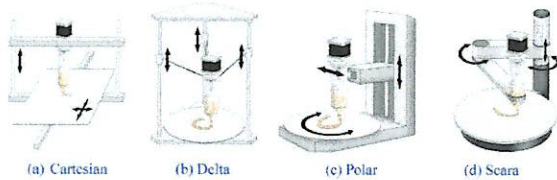


Fig. 3. 3D Printer structure types [3]

The 3D printer described in this paper is based on the linear delta structure, Kossel type (open source).

2. DESIGN REQUIREMENTS

The methodology for showcasing the differences between some of the most widely used 3D printing machine structures and their compliances regarding their performance expectations consist in mainly three phases: Firstly, the challenge was to identify some of the key specifications that define how 3D printers are required to perform. For this endeavor the

authors consulted the specialty literature and extracted 10 main specifications [4][5][6][7]:

- Printing speed (min. 100 mm/s);
- Accuracy (50 microns ±10);
- Printing volume (min. 250x220 mm);
- Layer thickness (100 microns ±10);
- Noise (55 db ±5);
- Printer’s size (max. 750x450 mm);
- Printer’s mechanism (delta);
- Printer’s source file ext. (.stl);
- Number of material colors (min. 1);
- Printing cost (max. 20 €/kg).

Secondly, the identified specifications were ranked using a widely employed instrument (AHP – Analytical Hierarchy Process), that prioritizes items, when they can’t be numerically compared and there are no objective criteria that can be used to compared them.

Criteria	Top Level ITEMS	Criteria	Criteria	Criteria	Criteria	Criteria	Criteria	Criteria				
	AHP Top-level Matrix											
	9: 0.50 an order of magnitude more important											
	8: 0.20 absolutely more important (6x as important)											
	7: 0.15 demonstrated more important (5x as important)											
	6: 0.10 demonstrated more important (4x as important)											
	5: 0.05 essentially more important											
	4: 0.03 essentially more important (3x as important)											
	3: 0.02 consistently more important											
	2: 0.01 twice as important											
	1.5: 0.007 somewhat more important											
	1: 0.005 equally important											
	0.7: 0.003 somewhat less important											
	0.5: 0.002 half as important											
	0.33: 0.001 clearly less important											
	0.25: 0.00075 essentially less important (other item 4x as important)											
	0.2: 0.0004 essentially less important											
	0.17: 0.17 demonstrated less important (other item 6x as impo...											
	0.14: 0.14 demonstrated less important											
	0.12: 0.12 absolutely less important (other item 8x as important)											
	0.11: 0.11 an order of magnitude less important											
		1: Printing speed (min. 100 mm/s)	2: Accuracy (50 microns ±10)	3: Printing volume (min. 250x220 mm)	4: Layer thickness (100 microns ±10)	5: Noise (55 db ±5)	6: Printer's size (max. 750x450 mm)	7: Printer's mechanism (delta)	8: Printer's source file ext. (.stl)	9: Number of colors (min. 1)	10: Printing cost (max. 20 €/kg)	importance in group
1	1: Printing speed (min. 100 mm/s)	0.2	0.33	0.33	5	5	0.33	3	0	0	7.7%	
2	2: Accuracy (50 microns ±10)		4	0.5	7	8	4	5	0	4	24.6%	
3	3: Printing volume (min. 250x220 mm)			0.33	6	2	0.2	3	4	3	6.4%	
4	4: Layer thickness (100 microns ±10)				8	8	0.2	0	7	5	19.2%	
5	5: Noise (55 db ±5)					2	0.14	2	3	0.2	2.8%	
6	6: Printer's size (max. 750x450 mm)						0.17	4	4	0.5	3.4%	
7	7: Printer's mechanism (delta)							8	0	8	25.8%	
8	8: Printer's source file ext. (.stl)								0.2	0.5	1.9%	
9	9: Number of colors (min. 1)									0.2	2.2%	
10	10: Printing cost (max. 20 €/kg)										4.3%	

Fig. 4. AHP – Delta Printer

Instead, this technique uses successive pairwise comparison between items (by devising an MxM matrix) to employ local objectification, enabling finally the expression of the importance of each item in the list, in percentage. It should be noted that by not comparing all the elements at once errors can be included in the matrix. However, for overcoming this drawback that authors also calculated the so called “consistency ratio” (CR). The specialty literature argues that a CR value less than or equal to 0.1 is deemed acceptable [8]. In our case the CR value was 0.073.

CR Value = 0.073 OK

Pairwise comparisons											
Item Number	Item Description	1	2	3	4	5	6	7	8	9	10
	Printing speed (min. 100 mm/s)	1.00	0.20	0.33	0.33	5.00	3.00	0.33	3.00	5.00	3.00
	Accuracy (50 microns ±10)	5.00	1.00	4.00	0.50	7.00	6.00	4.00	5.00	8.00	4.00
	Printing volume (min. 250x220 mm)	3.00	0.25	1.00	0.33	6.00	2.00	0.20	3.00	4.00	3.00
	Layer thickness (100 microns ±10)	3.00	2.00	3.00	1.00	8.00	8.00	0.20	9.00	7.00	5.00
	Noise (55 db ±5)	0.20	0.14	0.17	0.13	1.00	2.00	0.13	2.00	3.00	0.20
	Printer's size (max. 750x450 mm)	0.33	0.17	0.50	0.13	0.50	1.00	0.17	4.00	4.00	0.50
	Printer's mechanism (delta)	3.00	0.25	5.00	5.00	8.00	5.88	1.00	8.00	10.00	8.00
	Printer's source file ext (.stl)	0.33	0.20	0.33	0.11	0.50	0.25	0.13	1.00	0.20	0.50
	Number of colors (min. 1)	0.20	0.13	0.25	0.14	0.33	0.25	0.10	5.00	1.00	0.20
	Printing cost (max. 20 €/kg)	0.33	0.25	0.33	0.20	5.00	2.00	0.13	2.00	5.00	1.00
	Sum	16.40	4.58	14.92	7.87	41.33	30.38	6.38	42.00	47.20	25.40

Fig. 5. Pairwise comparison between technical specifications

Criteria	Printer types			Importance
	1 Cartesian structure	2 Delta structure	3 Polar structure	
1 Printing speed (min. 100 mm/s)	+	++	+	7.4%
2 Accuracy (50 microns ±10)	++	+	+	22.9%
3 Printing volume (min. 250x220 mm)	+	++	-	8.6%
4 Layer thickness (100 microns ±10)	++	+	+	20.0%
5 Noise (55 db ±5)	--	+	--	3.0%
6 Printer's size (max. 750x450 mm)	+	--	+	3.8%
7 Printer's mechanism (delta)	--	++	--	24.7%
8 Printer's source file ext (.stl)	++	++	++	1.9%
9 Number of colors (min. 1)	++	++	++	2.5%
10 Printing cost (max. 20 €/kg)	+	++	+	5.2%
Positive Effects	8	9	7	
Negative Effects	2	1	3	
Neutral Effects	0	0	0	
Net Effect	6	8	4	
Positive Priorization	55.6%	65.6%	24.2%	
Negative Priorization	-27.7%	-3.8%	-30.6%	
Net Effect	27.9%	61.8%	-6.4%	

Multicriteria Analysis	

Fig. 6. PUGH Matrix multicriteria analysis

Finally, a Pugh matrix was devised, having as inputs the ranked performance specifications and the 3D printing machine structures.

This instrument can be deployed in various formats, the authors proposed a version that is more commonly used: the set of criteria (on the left) constitute the probing questions or, in our case, the performance specifications, and the concepts to be selected are the machine structures (on the top). A scale from -3 to +3 was selected for completing the matrix, with the following significance: -3 strong negative effect (used symbol --), -1 some negative effect (used symbol -), 0 neutral (used symbol 0), +1 some positive effect (used symbol +), +3 strong positive effect (used symbol ++). These values are multiplied with the importance factor of each item (specification). The multiplied values are then summed up and the "Net Effect" is obtained, representing the proportional rating of each 3D printing machine structure, using the following formula:

$$\sum_{i=1}^n = \frac{\text{Importance of specification } n}{100} \quad (1)$$

* machine structure score n

3. THE DESIGN AND DEVELOPMENT OF THE 3D PRINTER

Printer design begins with modeling independent subsystems:

- Linear motion system;
- Power supply mechanism
- Arm rods;
- Rod heads, joints;
- Frame structure.

These systems include both standardized elements and uniquely designed parts specially designed to ensure the interconnection of standard elements. The 3D modeling and kinematic simulation of the printer was performed in Catia V5.

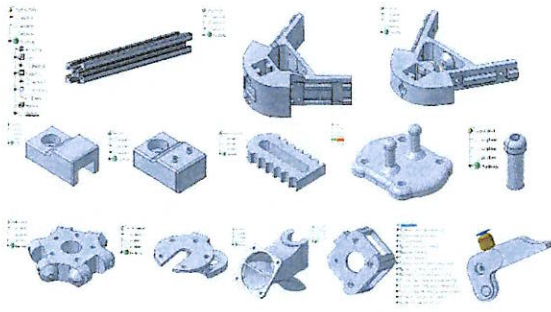


Fig. 7. CAD components of the Delta printer

The printer extruder is the subassembly that ensures the extrusion of the plastic filament (PLA, ABS, etc.). The designed extruder is similar to the one known on the market as Mk8, but has been modified to reduce the print head mass. Changes are made also in the area of wire extrusion area mainly on fixing the extrusion nozzle in the extruder body.

Having all the CAD models for the components and subassemblies, the 3D models were assembled (as seen in Fig 9) and simulated kinematically in Delmia V5 to check the workspace and possible collisions.

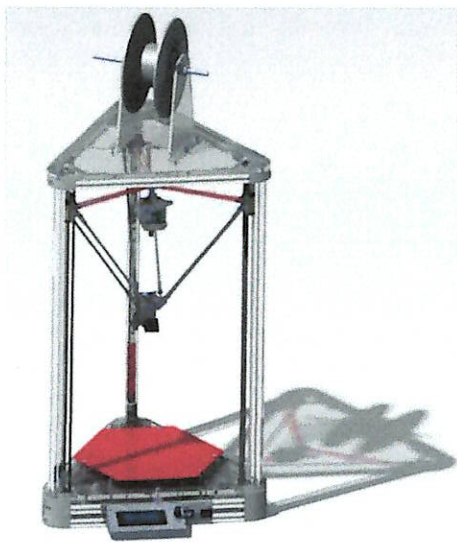


Fig. 9. The digital assembly of the printer

In addition to standardized components (guides, sensors, frame profiles, etc.), the other printer components were obtained by 3D printing.

Having all the mechanical components of the printer designed, the motors for operating the arms of the printer were dimensioned.

The total mass of the components to be driven by the engines is calculated by formula (2):

$$M_{total} = 3 * M_{carriage} + M_{arms} + M_{head} + M_{extruder} \quad (2)$$

$$M_{total} = 3 * 84g + 125g + 178g + 445g$$

$$M_{total} = 1000g$$

where,

M_{total} – total mass [g];

$M_{carriage}$ – carriage mass [g];

M_{arms} – arms mass [g];

M_{head} – printer head mass [g];

$M_{extruder}$ – extruder mass [g];

Calculation of the minimum power required for the engine to move the mass along the linear guide, in one second is the following:

$$F = m * g [N] \quad (3)$$

$$F = 0.350kg * 9.81 \frac{m}{s^2}$$

$$F = 3.4335 N$$

$$P = \frac{F * S}{t} [W] \quad (4)$$

where,

P - power [W];

F - force [N];

S - linear distance [m];

t - time [s]

$$P = \frac{3.4335 N * 0.5 m}{1 s}$$

$$P = 1.71675 W$$

The stepper motor chosen for the linear motion is Nema17, model 42HN47-1684A, being a hybrid motor, having the following characteristics: step angle 0.9 °, nominal voltage 2.8v, nominal current 1.65 A, phase inductance 2.8 mH, etc.

Having all the components of the printer defined, the printer can be assembled, calibrated and tested.



Fig. 10. The prototype of the Delta printer

The theoretical specifications of the printer calculated based on the mechanical characteristics are:

- max rot/s: 0.76;
- max rot/min: 45.45;
- maximum power: 4.62 W;
- minimum step time: 3.30 ms;
- ideal voltage: 53v;
- belt steps/mm: 160;
- step resolution: 0.1 mm;
- micro step resolution: 0.00625 mm;

4. RESULTS

The printer's resolution can be calculated using one of the following equations:

$$\text{printer resolution} = \frac{1}{\text{steps/mm}} = \dots \text{mm} \quad (5)$$

or

$$\text{printer resolution} = \frac{1000}{\text{steps/mm}} = \dots \mu\text{m} \quad (6)$$

where,

$$\frac{\text{steps}}{\text{mm}} = \frac{\text{motor steps} * \text{driver microsteps}}{\text{pitch of belt} * \text{pulley teeth}} \quad (7)$$

To start the calibration procedure, a manual pre-calibration of the printer was performed using the paper sheet method in the following points:

- Origin (0,0,0);
- Column X (-77.94, -45,0);
- Column Y (77.94, -45,0);
- Column Z (0, 90,0);

Using the open source utility "Delta Kinematics Calibration Tool" and an inductive sensor mounted in the print head, successive point measurement interactions were performed:

origin, X column, x_opposite, Y column, y_opposite, Z column, z_opposite, final values of the interactions obtained with the "Delta Kinematics Calibration Tool" are written in the printer's EPROM and will continue to be used as the default parameters. After the printer was calibrated, it was tested. This test consisted of printing cubes with a side of 20 mm, and a wall thickness of 3 mm. This piece is shown in the figure below.



Fig. 11. Printed testing cubes

Three of the faces were marked with X, Y and Z, the average of the values obtained for 35 measurements is 19.71 mm for X, 20.05 mm for Y and 20.10 mm for Z. The figure below shows the histograms for each of the 3 faces.

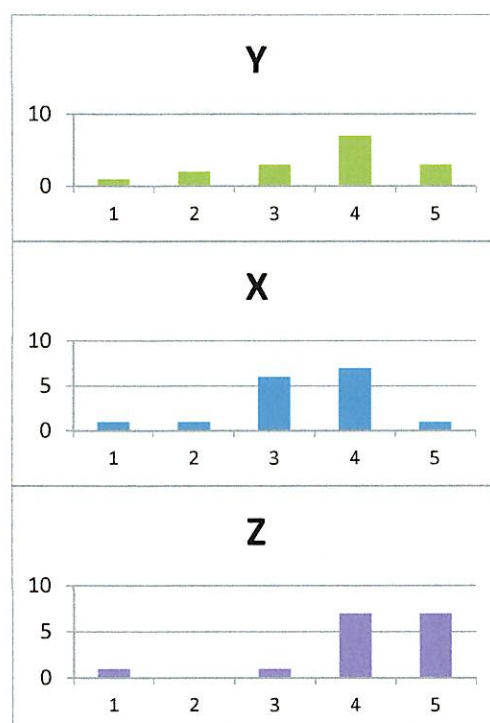


Fig. 12. Measurements of the testing cubes

After analyzing the measurements made with a micrometer, we can say that the dimensional accuracy is ± 0.2 mm.

8. REFERENCES

- [1] A. E. Jakus, "An Introduction to 3D Printing—Past, Present, and Future Promise," in *3D Printing in Orthopaedic Surgery*, Elsevier, 2019, pp. 1–15.
- [2] "Global 3D printing products and services market size from 2020 to 2024," 2020. [Online]. Available: <https://www.statista.com/statistics/315386/global-market-for-3d-printers/>. [Accessed: 11-May-2020].
- [3] J. Sun, W. Zhou, D. Huang, and L. Yan, "3D food printing: Perspectives," in *Polymers for Food Applications*, Springer International Publishing, 2018, pp. 725–755.
- [4] T. Ludwig, O. Stickel, A. Boden, and V. Pipek, "Towards sociable technologies: An empirical study on designing appropriation infrastructures for 3D printing," in *Proceedings of the Conference on Designing Interactive Systems: Processes, Practices, Methods, and Techniques, DIS*, 2014, pp. 835–844.
- [5] J. ten Kate, G. Smit, and P. Breedveld, "3D-printed upper limb prostheses: a review," *Disabil. Rehabil. Assist. Technol.*, vol. 12, no. 3, pp. 300–314, Apr. 2017.
- [6] A. Pîrjan and D.-M. Petroșanu, "The Impact Of 3d Printing Technology On The Society And Economy," *J. Inf. Syst. Oper. Manag.*, vol. 7, no. 2, pp. 360–370, 2013.
- [7] M. E. and B. R., "3D printing: On its historical evolution and the implications for business," in *Portland International Conference on Management of Engineering and Technology (PICMET)*, 2015, pp. 551–558.
- [8] R. W. Saaty, "The analytic hierarchy process-what it is and how it is used," *Math. Model.*, vol. 9, no. 3–5, pp. 161–176, Jan. 1987.

PROIECTAREA ȘI REALIZAREA STRUCTURII UNEI IMPRIMANTE 3D DELTA LINIAR

Rezumat: Lucrarea prezintă procesul de proiectare și dezvoltarea unei imprimante liniare Delta 3D. Structura mecanică cea mai frecvent utilizată pentru imprimantele 3D care utilizează depunere prin fuziune (FDM) se bazează pe mecanismul tradițional paralel. Această lucrare evidențiază avantajele unei imprimante 3D cu structură Delta în comparație cu structurile carteziene cu privire la diferite specificații tehnice, cum ar fi precizia, viteza de imprimare, grosimea stratului și dimensiunea totală a imprimantei. Instrumentele AHP au fost utilizate pentru a identifica designul optim al imprimantei și a fost concepută o matrice PUGH pentru a obține cel mai bun clasament al structurilor de imprimare 3D posibile. Precizia imprimantei dezvoltate a fost comparată cu alte imprimante carteziene disponibile pe piață pentru a evidenția precizia asociată cu viteza de imprimare a imprimantei Delta 3D.

Raul-Silviu ROZSOS, Department of Design Engineering and Robotics, Technical University of Cluj-Napoca, Romania, raul.rozsos@muri.utcluj.ro

Zsolt Levente BUNA, Department of Design Engineering and Robotics, Technical University of Cluj-Napoca, Romania, zsolt.buna@muri.utcluj.ro

Ștefan BODI, Department of Design Engineering and Robotics, Technical University of Cluj-Napoca, Romania, stefan.bodi@muri.utcluj.ro

Radu COMES, Department of Design Engineering and Robotics, Technical University of Cluj-Napoca, Romania, radu.comes@muri.utcluj.ro

Vasile TOMPA, Department of Design Engineering and Robotics, Technical University of Cluj-Napoca, Romania, vasile.tompa@muri.utcluj.ro

MANUFACTURING METHOD FOR BICYCLE SADDLE FROM CARBON/EPOXY COMPOSITE MATERIALS

PAUL BERE^{1*}, RAUL ROZSOS², CRISTIAN DUDESCU³, CĂLIN NEAMȚU²

Abstract. The fiber reinforced polymer in the last decades had a very impressive development. Currently, it is used in almost all of the areas from fashion to aerospace. In this paper, a new method is proposed for design and manufacture of bicycle seat post from carbon fiber reinforced polymer (CFRP) Starting to design piece, to final prototype by CFRP is presented. The design procedure using an anatomical analysis of the ischioion bone and the cycling position are presented. In the seat post design CATIA V5 packages was used, where finite element analysis of the applied loads was performed, as well. The manufacturing method using autoclave curing and vacuum bag technology to obtain the seat post prototype from CFRP was presented. The weight of bicycle seat post obtained is 43 grams and 73 grams including the fixation bars. This represented 4 times lighter like plastic/leather performance saddle. Using this method the number of the CFRP layers and the corresponding reinforced materials architecture were determined.

Key words: bicycle saddle, Carbon fiber reinforced polymer, composite materials.

1. INTRODUCTION

During the last decades, bicycles benefited manufacturing of several parts produced out of very sensitive, light, special, and ultra-performance materials. One of these categories is fiber reinforced polymer (FRP), which finds rapidly growing application area. Migrated from aerospace domain practically, FRP materials covered a wide domain, bringing special properties to the component. Several authors studied special applications of FRP materials, from medicine to aviation, from Formula One to wind turbine, enabling FRP materials to continue becoming a dominant material in the entire product design and manufacture domain. Dziejczak et al. in [1] studied application of FRP materials on dental industry, where they focused on the tribological properties of the FRPs.

¹ Technical University of Cluj-Napoca, Department of Manufacturing Engineering, Bd. Muncii 103-105, Romania

² Technical University of Cluj-Napoca, Department of Design Engineering and Robotics, Bd. Muncii 103-105, Romania

³ Technical University of Cluj-Napoca, Department of Mechanical Engineering, Bd. Muncii 103-105, Romania

* Corresponding author: Paul Bere

The application of FRPs in aviation industry is related in [2]. The author proposed to use continuous carbon-fibre-reinforced/poly-ether-ether-ketone (CCF/PEEK) composites for manufacture of complex structural parts in aerospace to replace metal components. From bicycle application the authors studied the frame design [3]. The fiber direction and stacking sequence design for the bicycle frame were analyzed. They traded the load application from theoretical point of view, where the experimental verification and manufacturing practices were missing. 3D printing of carbon fiber reinforced polymer (CFRP) is presented in [4]. The mechanical properties of the CFRP and the FDM process parameters were investigated. They used in this case a thermoplastic material for matrix, and CFRP powder material. The effects of process parameter on the tensile properties of materials are investigated.

In [5–7] comfort the authors treated the cyclist's based on vibration determination. Position on the bike during seated sprint cycling is evaluated in [8,9]. The authors studied the optimization of lower limb joint kinematics while participants undertake sub-maximal intensity cycling.

In this paper, it is aimed to propose a new design for race bicycle saddle. This new prototype brings a CFRP lighter piece and a comfortable position of the rider. Starting from market trends, human anatomy, and new manufacturing processes, a new model made from carbon fiber/epoxy reinforced polymer (CFRP) is proposed. The design stages for the new geometry were performed using the Catia V5 software package. In order to make a CFRP piece, a rigid mold is required. The CFRP is applied in the unpolymerized state on this mold. The CFRP is pressed in the mold cavity and polymerized at a certain temperature, through various manufacturing processes. After the polymerization, CRFP is removed from cavity mold, so that the composite part is obtained. In general, molds are devices that have high costs due to complex surface processing. There are several ways and materials for mold manufacturing. The important specifications for molds are the cost, the manufacturing time, the dimensional precision obtained, and the lifetime.

The solution chosen for mold manufacturing assumes to use of a rapid prototyping (RP) process. In our case using a master model realized by Fused deposition modelling (FDM) technology and a composite mold were done. The FDM process is not relatively new, its use in fast master model making from different plastic polymers. In the manufactured mold, a new seat post of bicycle was manufactured from CFRP Prepreg.

2. DESIGN AND THE MANUFACTURING METHODOLOGY OF THE BICYCLE SADDLE

2.1. Design of the new prototype

In the design of the seat post, its fastening element was considered in accordance with the bicycle production standards. More specifically, the position



of the cyclist should be as comfortable as possible and the seat post to be lighter and more rigid. It was considered the fact that performance cyclists are of low height (160–175m) and generally people that weighing up to 70 kg. Thus, the design was performed to carry a maximum weight of 80 kg. For heavier cyclists, additional layers of composite material can be applied to provide proper mechanical characteristics. The bicycle seat post model corresponds to the movements and demands for a circuit on the road. Following discussions with performance cyclists, they have shown interest in making the bicycle seat post as rigid as possible, so that all their energy is transferred to the pedals. The shock absorption to the anatomical parts of the body is achieved by the protection (sponge) placed in the pants used in cycling.

For the current bicycle seat post, a size of 12 was chosen, that is, a width of 120 mm and a length of 250 mm. It is noteworthy to state that, the size does not provide comfort for every individual because the position of the ischion bone differs from one person to another. In some cases, other sizes may be used that provide a greater or lesser width of the seat depending on the anatomical position of the cyclist.

Starting from the anatomy of human bones and the position of the cyclist on the bike, a curve defining the contact points of the cyclist with the top has been set in the longitudinal plane. The same was done in the transverse plane, considering the pressing of the lower bones of the pubis on the contact surface (Fig. 1).

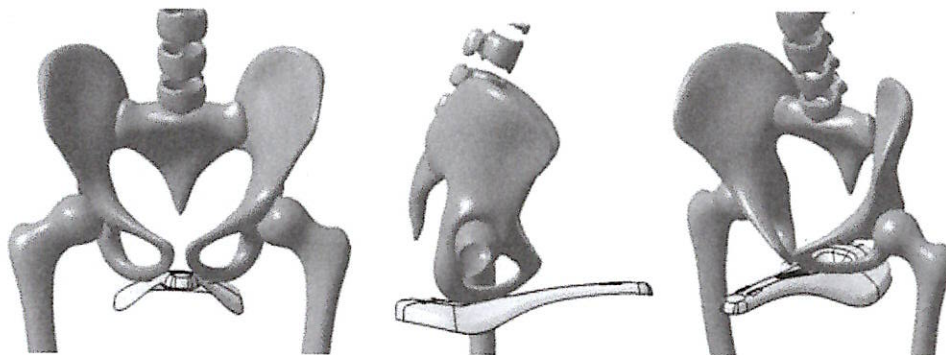


Fig. 1 – Determination of the longitudinal and transverse curves of the bicycle saddle.

Then, the fixing area of the two bicycle seat rods that fixes the seat position the center rod is set. After the two curves were generated and the fixation area of the two rods was established, it went on to create the new model of the bicycle seat. After setting the outer shape (Fig.2a) on the central part a longitudinal middle channel (Fig.2b) was made to release the pressure on the prostate if the cyclist is male.

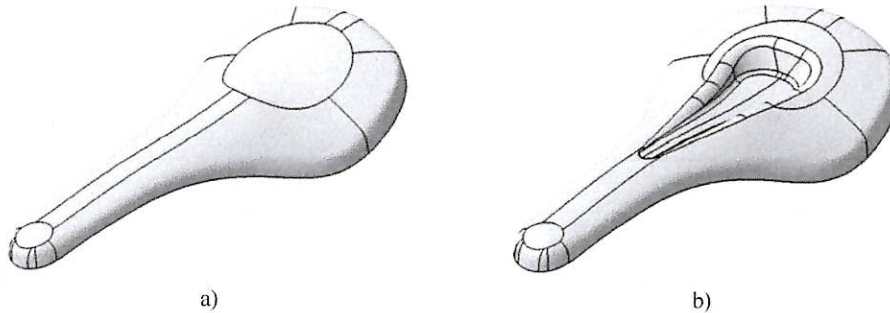


Fig. 2 – Bicycle seat post CAD model.

By making a longitudinally disposed cavity in the middle of the cyclist's area, the pressure applied to the prosthesis during pedaling was eliminated. When designing the new model, the problems that may occur in the lower zone of the basin's bones and in the perineum area were considered. It was desired to release the pressure generated in the area of the pubic arch and the pressure in the area of the tissues that make up the perineum. It should be noted that this model is customized only for some individuals with the anatomical configuration and basal bones specific to the design conditions.

2.2. Designing and manufacturing of the mold

Reducing bike mass is the main objective for performance cycling. Therefore, it has been chosen to manufacture the bicycle seat post made of CM. This being the main objective, it was chosen to make bicycle seat post using CFRP. The CFRP benchmarking technology involves manufacturing the piece in a mold using certain manufacturing processes. To obtain maximum mechanical characteristics, it was chosen to manufacture the CFRP piece by the vacuum bag forming process.

In order to reduce the manufacturing time of the new bicycle seat post prototype, a new solution was chosen. The solution is making a mold as quick as possible. A plastic master model using the CAD designed prototype was manufactured. This rapid manufacturing process greatly reduces manufacturing time and saddle costs. Considering the fact that the FDM process produces a surface of parts with a certain roughness that is not suitable for the manufacture of CFRP mold, it was considered that the active part of the prototype was coated with a gelcoat layer which will then be machined until polishing the active surface of the master model.

For this, an ABS thermoplastic material was chosen to be used in order to make the RP of the saddle. This material is sensitive to solvents from polyester gelcoat and makes very good coupling between these two materials.

To obtain the bicycle seat post from CFRP, several mold design variants have been considered. The simplest option involves making a master model piece, and making a composite mold using the master model piece. The method consists in using a rigid master model of the piece. This will be covered by different CM in order to obtain a rigid mold. The methodology supposed to have an additional step in manufacturing process and this is master model manufacturing.

In order to eliminate this step, it is possible to consider designing a CNC milling machine from an Epoxy or Aluminum block. The process involves high manufacturing costs in milling, material and subsequent processing. Molds made of metal blocks are generally for large series of manufacturing. Thus, a method of making the molds by rapid prototyping master model and composite mold was chosen. Generally, the CFRP pieces are made larger at the edge to avoid areas where the fabric is falling apart. This additional part is cut at the end, producing a composite material with a structure of the homogeneous reinforcement material at the edge. Taking this into account, the area of the bicycle seat has been extended by 10 mm. A separation plane was established in the edge area and the whole surface was integrated into a material block, obtaining a cavity (Fig.3). A surface check was performed in the mold design phase to determine possible complex geometries or negative angles that could prevent piece extraction from the mold.

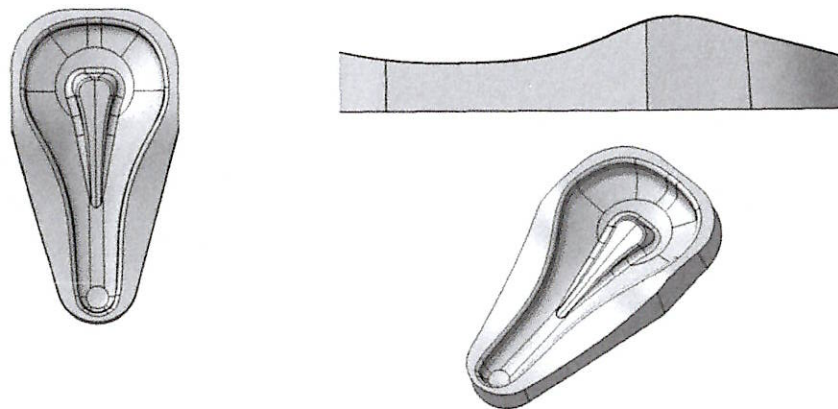


Fig. 3 – The CAD model of the mold.

An inspection was done to ensure there are no corners or planes between which there is an angle of less than 90° . At intersections between the planes, connecting rays were applied. Thus, CFRP can be applied without creasing.

The printer used to manufacture this master model was the LeapFrog printer, the Creart HS XL model; its print size is $280 \times 270 \times 590$, being able to print multiple pieces in the same piece. Due to the size of the machine table the master

model of the saddle was arranged on the machine table. To create the G slicing code used to make the prototype; we used the Ultimaker software, Cura 4.0.

The material used to manufacture the saddle is ABS LEAPFROG MAXX Essentials. The material is provided by the manufacturer of the 3D printer. The printing temperature was 245 for the material and 80 for the printer heated bed, 1.75 mm filament thickness, 0.4 mm extruder head nozzle diameter.

The CURA 4.0 software has estimated the printing time, more specific: 38 hours and 43 minutes. The layer thickness is 0.2 mm, and as the internal structure of the piece we have: wall thickness: 4 layers; piece infill (filling): 75%; structure of infill "grid". The printing speed is 60 mm/s. For printing the exterior wall, a lower speed of 30 mm/s was chosen to achieve better dimensional accuracy and roughness.

After the master model was manufactured by RP, in order to improve the quality surface a layer of T35 Polyester Gelcoat was applied on the active side of the prototype. This procedure was through spraying, and the polymerization was made in the oven at 50° C for 4 hours. The active surface of the FDM prototype was machined with abrasive paper having from 80 grit to 1200 grit. The procedure was followed by polishing with 1 μm diamond paste solution. In Fig.4 the master model of the saddle are presented.

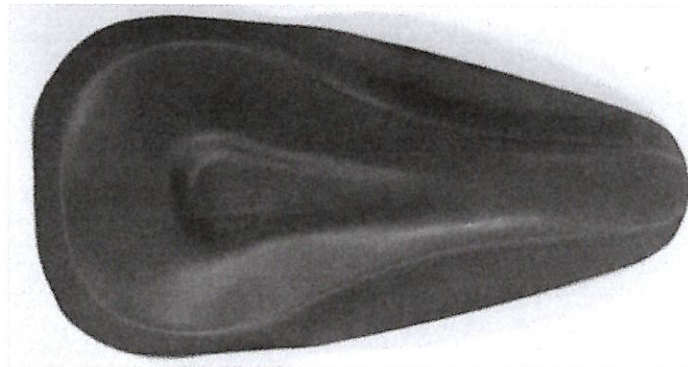


Fig. 4 – Master model of the bicycle saddle manufactured by FDM process.

Using this prototype a CM mold were done. The surface of the prototype was covered by different CM in epoxy matrix. On the surface of the prototype 5 layers of release agent in order to prevent the adhesion of composite to saddle prototype surface were applied. Different layers by glass fiber/epoxy using hand lay-up technology were applied on obtained prototype in order to obtain a CM mold. The mold was introduced in the oven for polymerization. The temperature cycle was 40°C – 8 hours', 60°C – 8 hours' time. Considering the temperature at which the mold is exposed during CFRP polymerization, additional treatment was applied at 110°C for 8 hours.

2.3. Simulation and design of composite material for the manufacture of bicycle saddle

In order to determine the stress level and the proper stacking sequence of the CFRP layers a FE analysis of the saddle were performed. Were used ANSYS Workbench software. The FE analysis considers the bicycle seat loaded under the forces of given by the cyclist weight. The boundary conditions are presented in Fig. 5. The boundary conditions in form of fixed supports have been applied to the seats in the area of support bars that connect the structure with the bicycle frame. A total force of 800 N is applied on upper faces in contact with the human body.

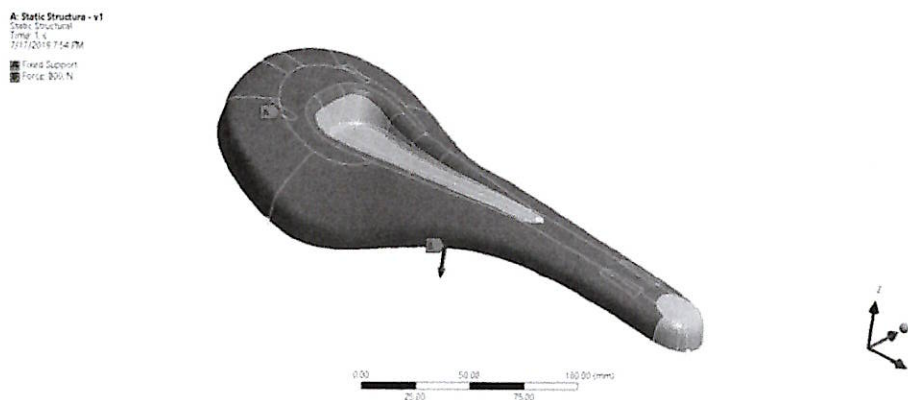


Fig. 5 – Static load application.

The composite material has three layers with the following stacking sequence $[0/90/+45/-45/0/90]$ and is made of twill fabric with a density of 240 g/m^2 . The values of elastic constants obtained by experimental tensile tests of composite samples are: $E_x=79\,505 \text{ MPa}$, $E_y=78\,915 \text{ MPa}$, $G_{xy}=35\,433 \text{ MPa}$ and Poisson ratio, $\nu=0.268$. From the point of view of the material, a conclusion shows us that the two-layer orchid made of two layers of T245 material does not withstand the stresses.

In Fig.6 is presented the total displacement of the bicycle seat for the two geometrical variants. The maximum principal stress is shown in Fig.7. The stress values are higher in the fixation areas, which were additionally fixed by gluing the fixation frames. As a general observation it can be noticed that the full seat is stiffer than the seat with the median channel.

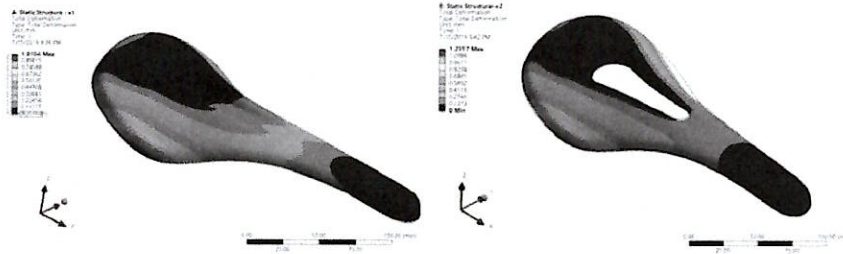


Fig. 6 – Total displacement.

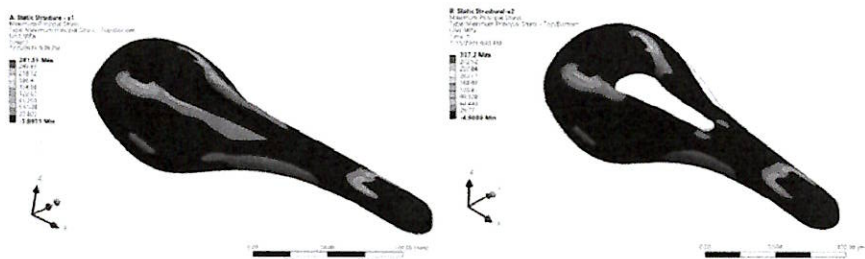


Fig. 7 – Maximum principal stress.

2.4. Manufacturing of the prototype from CFRP

Materials used. For the manufacture of CFRP parts, prepreg material type GG245T-DT806W-42 was used from the DeltaPreg part of Toray Group. The fabric consists of a twill fabric (T) by 245g/m² carbon fiber. The epoxy matrix is type DT 806W and weight fraction ratio of resin is 42%. This matrix can also be used for oven polymerization processes without requiring polymerization in the autoclave at high temperature. The polymerization process according to the manufacturer's specifications allows polymerization at different temperatures as indicated in Table 1. The producers are recommended cycles up to 120°C.

Table 1

The producers are recommended cycles up to 120°C

Cure Cycle	Time [Hours]	Temperature [°C]	Time [Hours]	Temperature [°C]
Cycle	16	65	1,5	100
Cycle	10	70	1.0	110
Cycle	5	80	1.0	120
Cycle	3	90		

We had an option to choose one of this cure cycle to polymerized this type of resin. Preparing the mold was performed by applying successive layers of release agent LOCTITE@FREKOTE700-NC™ type. Ten coats were applied by means of a cotton swab. Drying time between layers was 20 minutes at 20° C. After drying each layer the surface was polished. The prepreg composite material was removed from the freezer at -17° C and kept at 20° C for 24 hours. The application of the prepreg composite material has been achieved layer by layer (see Fig.9) by hand lay-up procedure. The material was heated to 40 degrees to avoid creasing using a portable industrial blow dryer at 40° C on the areas that had a more complex geometry.



Fig. 9 – Application of CFRP layers on the mold.

After the first layer of CFRP applied on the mold cavity, a vacuum pressure was applied to -0.9 bar. The CFRP applied on the mold was covered with a release film and a layer of Peel Ply. After that, the mold and first composite layer was placed in a vacuum bag where -0.9 bar was applied over 30 minutes. The procedure helps to stick and remove air bubbles from the surface of the mold, especially in the area of complex surfaces or corners.

After finishing this treatment, the next step is to apply the other layers according to the results set in the design phase of the material.

Three CFRP T 240 layers by sequence [0-90 / ± 45/0-90] were used in the present case. The CFRP prepreg mold assembly was covered with a release film and a breather fabric. The Assembly was inserted into a vacuum bag. It was sealed to the edges and with a vacuum coupled a vacuum pressure of -0.9 bar for 30 minutes at 20 ° C was applied (Fig.10). CFRP polymerization was done in the oven at 90° C for 24 min. After polymerization, the part was removed from the mold. Its outer surface was observed to be non-porous with well material compaction.



Fig. 10 – Applying vacuum pressure through mold and composite material.

In order to obtain the same dimension of the CFRP prototype the excess of the border were cut. The surface was processed by glass paper from 400 grit.

3. RESULTS AND DISCUSSIONS

3.1. Design of the saddle results

Designing the new seat post for high performance bicycle using the new design methods greatly reduces manufacturing time. The new proposed concept considers the health issues that an incorrectly designed bicycle seat could cause. A new concept has been sought that could improve the design to eliminate. One of this problem is the geometry of the saddle are not comfortable or not proper for cyclist. Other problems are dimension of the saddle or the geometry. This can applied the pressure on the prostate gland.

A RP method and a new material were chosen in order to create the master model prototype and a composite mold to obtain CFRP piece. The manufacture of the ABS saddle prototype offers the possibility of machining the active part of the

piece. On the obtained surface, gel coat layers can be applied and then can be polished. Thus, the polished area is a perfect surface that provides an area where CFRP does not adhere to this surface. Not all the thermoplastic materials can be use from this considering.

3.2. Manufacturing of the prototypes results

The obtained roughness on the active surface of the saddle prototype after machining on FDM was $R_a = 0.2$ mm and after application of the polyester gelcoat layer and it's processing $R_a = 0.05$ μm .

The obtained mold made by CM is shown in Fig. 10. This is used to manufacture the bicycle seat prototype in CFRP.

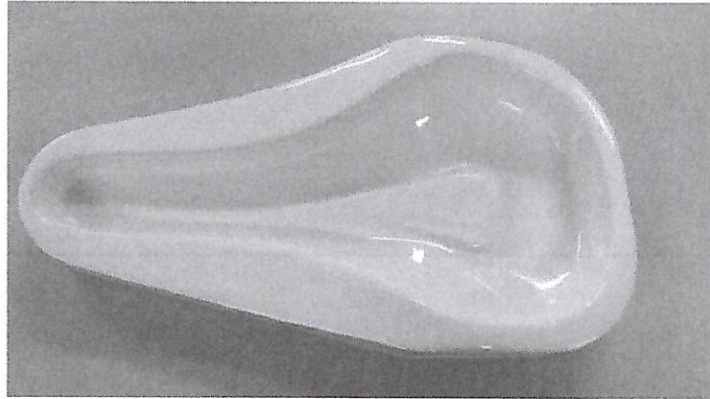


Fig.10 – Composite mold obtained by hand lay-up technology.

The obtained bicycle saddle has a mass of 43 g. Subsequently, using a 3M™ Scotch-Weld DP 420 structural adhesive, the fixing rods are glued. In Fig.11 are presented the obtained CFRP bicycle saddle.

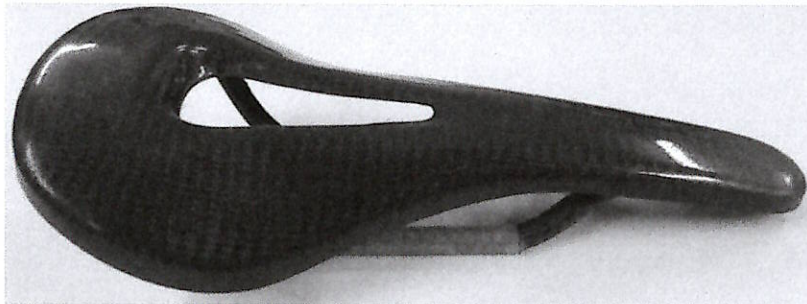


Fig.11 – The CFRP saddle obtained.

3.3. Economical analysis

Considering the amount of material estimated by the Ultimaker software, Cura 4.0, that is, 595 g of material used, this is consistent with the prototype obtained. The cost price on the market for the respective benchmark of 11 Euros / 100 g of material can be calculated as an estimate. The estimated cost of the mold made through FDM prototype and CM mold is 100 euro. The outer surface of the CFRP is glossy copying the surface of the mold. No areas with defects or excess resin are observed.

An important factor to underline is the behavior of the CM mold made by CM that did not suffer deformations by exposing it to temperature and pressure. This was measured and the initial dimensions correspond to the original dimensions. No cracks or deformations in the active area of the mold are observed. Twenty pieces with different configurations of the reinforcement material were made for their testing.

The CNC milling machines of the mold, having an operation cost of 25 to 45 Euros/hour. It's takes about 12 hours, which costs minimum of 400 euros of machining cost including the material. This is a significant reduction in mold preparation when the mold material is CM.

In aluminum case of the mold the estimate weight is 2 000 g. The CM obtained mold has 600 g including Gelcoat layer.

3.4. Dimensional measurements

The dimensional evaluation of the CFRP seat post made in the CM mold was done using a portable co-ordinate measuring machine (Fig. 13).



Fig. 13 – Dimensional evaluation of CFRP seat post.

The comparison between real part and CAD model was made in 131 points acquired manually in various areas of the bike saddle as shown in Fig. 14, where the green color represents a very small difference between the CAD model and the real one as the shades go to the blue it the difference increases. Figure 15 shows the deviation of the points from the nominal size (top) and the normal distribution of errors of physical model related to the CAD model.



Fig. 14 – Points acquired on CFRP seat post.

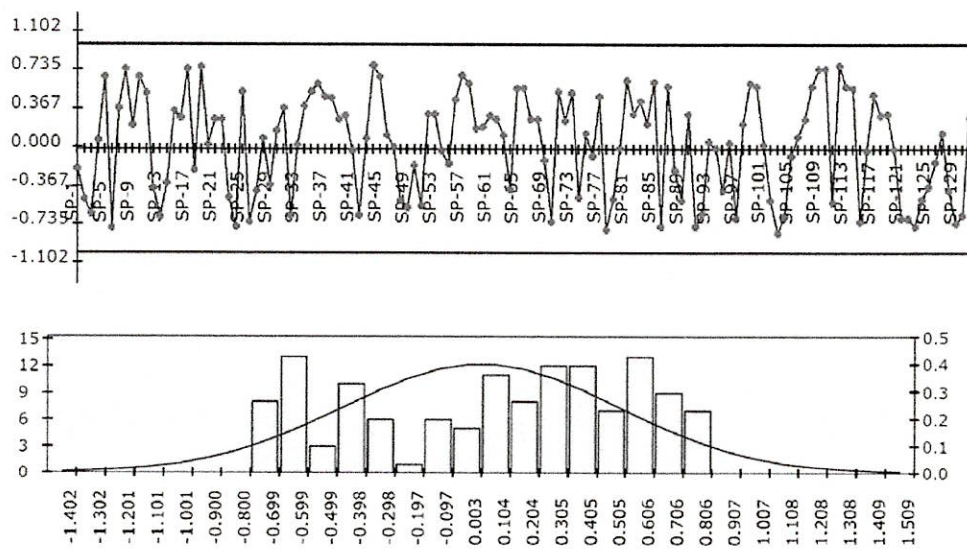


Fig. 15 – Deviation of the points from the nominal dimension (top) and the normal distribution of the physical model errors to the CAD model (bottom).

The differences between the real part and CAD models in ranges of ± 0.8 mm, considering these deviations and the functional role of the part it can be stated that the piece is dimensionally precise. The difference between CAD model and final CFRP saddle prototype can be attributed to the layer of gelcoat applied to the FDM saddle prototype surface and in the same time, surface processing preparation.

5. CONCLUSIONS

Applied on CFRP in high performance bicycle components bring a lot of benefits. The most important are the mechanical behavior and weight of the components.

The new application of the RP technologies in the CM manufacturing process reduced the cost of the mold by 4 times compared CM mold by CNC aluminum milling mold.

The weight of CM mold is 3.36 times lower like aluminum case. The obtained CM mold can be used to prepare the CFRP components. Twenty pieces were obtained and the mold is not affected, it can be used for a next pieces.

The FE analysis using the ANSYS software indicates the 3 layers of the CFRP for the final piece. Different stacking sequence of the layers can be applied to obtain a comfortable cyclist position and the elastic deformation. Depends of the road the saddle must to absorb a little the vibration coming from a bumpy road.

The standard deviation between CAD model and obtained CFRP saddle is in ranges of ± 0.8 mm. Considering the application of the piece this can be dimensionally precise. The precision can be improved in the designing stage considering the gelcoat layer dimension. We must to mention that this mold solution is proposed for prototyping of CFRP piece.

The lifetime of the aluminum mold can be not compared by CM mold. This mold can be applied in the mass production case.

The weight of the obtained bicycle saddle is 75g including the fixing bars, which is 4 times lighter like plastic/leather performance one.

Received on June 29, 2019

REFERENCES

1. DZIEDZIC, K., ZUBRZYCKA-WROBEL, J., JOZWIK, J., BARSZCZ, M., SIWAK, P., CHALAS, R., *Research on tribological properties of dental composite materials*, Advances in Science and Technology–Research Journal, **10**, 32, pp. 144–149, 2016; DOI: 10.12913/22998624/65123.
2. LUO, M., TIAN, X.Y., SHANG, J.F., ZHU, W.J., LI, D.C., QIN, Y.J., *Impregnation and interlayer bonding behaviours of 3D-printed continuous carbon-fiber-reinforced poly-ether-ether-ketone composites*, Composites Part a-Applied Science and Manufacturing, **121**, pp. 130–138, 2019; DOI: 10.1016/j.compositesa.2019.03.020.

3. LIU, T.J.-C., WU, H.-C., *Fiber direction and stacking sequence design for bicycle frame made of carbon/epoxy composite laminate*, *Materials & Design*, **31**, 4, pp. 1971–1980, 2010.
4. NING, F.D., CONG, W.L., HU, Y.B., WANG, H., *Additive manufacturing of carbon fiber-reinforced plastic composites using fused deposition modeling: Effects of process parameters on tensile properties*, *Journal of Composite Materials*, **51**, 4, pp. 451–462, 2017; DOI: 10.1177/0021998316646169.
5. AYACHI, F.S., DOREY, J., GUASTAVINO, C., *Identifying factors of bicycle comfort: An online survey with enthusiast cyclists*, *Applied Ergonomics*, **46**, pp. 124–136, 2015; DOI: 10.1016/j.apergo.2014.07.010.
6. BINI, R., DALY, L., KINGSLEY, M., *Changes in body position on the bike during seated sprint cycling: Applications to bike fitting*, *Eur. J. Sport Sci.*, pp. 1–8, 2019; DOI: 10.1080/17461391.2019.1610075.
7. DORIA, A., MARCONI, E., ASME, *A testing method for the prediction of comfort of city bicycles*, *Proceedings of the Asme International Design Engineering Technical Conferences and Computers and Information in Engineering Conference*, Vol. 3, 2018.
8. BINI, R., HUME, P.A., CROFT, J.L., *Effects of bicycle saddle height on knee injury risk and cycling performance*, *Sports Medicine*, **41**, 6, pp. 463–476, 2011; DOI: 10.2165/11588740-000000000-00000.
9. GARCIA-LOPEZ, J., RODRIGUEZ-MARROYO, J.A., JUNEAU, C.E., PELETEIRO, J., MARTINEZ, A.C., VILLA, J.G., *Reference values and improvement of aerodynamic drag in professional cyclists*, *Journal of Sports Sciences*, **26**, 3, pp. 277–286, 2008; DOI: 10.1080/02640410701501697.



TECHNICAL UNIVERSITY OF CLUJ-NAPOCA

ACTA TECHNICA NAPOCENSIS

Series: Applied Mathematics, Mechanics, and Engineering
Vol. 61, Issue Special, September, 2018

USING COMPOSITE MATERIALS FOR DASHBOARD DESIGN OF AN ELECTRIC CAR

Sergiu SOLCAN, Calin NEAMTU, Paul BERE, Rares GHINEA, Raul ROZSOS, Attila PAPP

Abstract: The paper presents a dashboard made integrally of composite materials designed for an electric car with two passengers. There are presented and analyzed the possibilities of realization of the dashboard, as well an optimized model of the dashboard that can be made entirely of composite materials.

Key words: composite materials, dashboard design, electric car, micro car

1. INTRODUCTION

Composite materials are used in dashboards, especially for sports cars or luxury cars. It is usually used to cover the dull portions of the dashboard (Figure 1) with more of a decorative role, but it can also be found on other elements inside the passenger compartment, such as the steering wheel, the gearshift or the interior of the doors.



Fig.1 Composite material on Tesla Concept dashboard [1].



Fig. 1 BMW Car Dashboard Design [2].

The dashboard design is a subject approached from various points of view like:

- Usability - use of automotive user interface technology, and specifically, to explore the instrument panel (IP) display design to help attract and manage attention and make information easier to interpret [3],
- Fabrication technology – starting with design of injection mold [4], influence of manufacturing constraints on the topology optimization of an automotive dashboard [5],
- Ergonomics - in terms of driving safety and accessibility to the dashboard control elements [6],

and others.

In designing and optimizing dashboards various tools are used such as: design evaluation model (DEM) and analytic hierarch process (AHP) [6], augmented reality [7], topology optimization (TO) [5], TRIZ method and Multi Criteria Decision Method (MDCM) [8].

In this paper we propose an analysis of the possibilities of realizing a dashboard entirely of composite materials.

2. 96BG E-CAR CONCEPT

The 96BG concept is a small electric car designed to be used in crowded cities, designed

for day-to-day activities and has two seats to meet a wide range of users. The design is a modern one, as can be seen in the figure below, the shapes used in its 3D modelling are adapted to the FPR parts manufacturing technology.



Fig. 2 96BG E-CAR concept.

3. DESIGN ALTERNATIVES

Most composite dashboards are made of a single piece and are conceived as spare parts, copying the design of an existing dashboard.



Fig. 3 Dashboard made of composite material [9]

In this paper three design variants will be presented (see Figure 5), differentiated by the method in which the dashboard will be assembled. For each method the strengths and weaknesses will be highlighted, extracted from a SWOT analysis.

In the first concept the dashboard is made from a single piece, in the second one there is a part that can be considered the cover for the other components, and in the case of the third concept components are mounted one above the other.

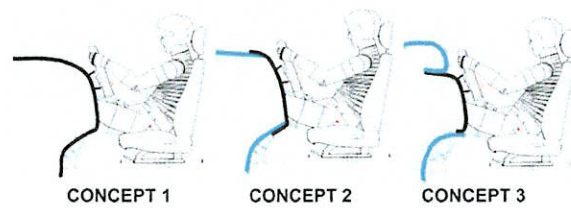


Fig. 4 The three concepts analysed

3.1 Concept 1

The first option in designing a dashboard is to do it in from one piece (Figure 4).



Fig. 5 Design 1

Using the SWOT analysis presented in Figure 7, a number of problems have been identified with the design of the mold and its assembling into the vehicle. By making one-piece dashboard, the sounds created by wearied-out plastic under stresses are eliminated. As a weakness we can recall the difficulties that may arise during the assembly process, the piece being too large or the high cost and the complexity of the dashboard mold.

3.2 Concept 2

Concept number two (Figure 8) involves building a three-component dashboard, one of which covers the other two (or more) components. On this top cover are mounted the panel of instruments and the ventilation holes.



Fig. 6 SWOT analysis

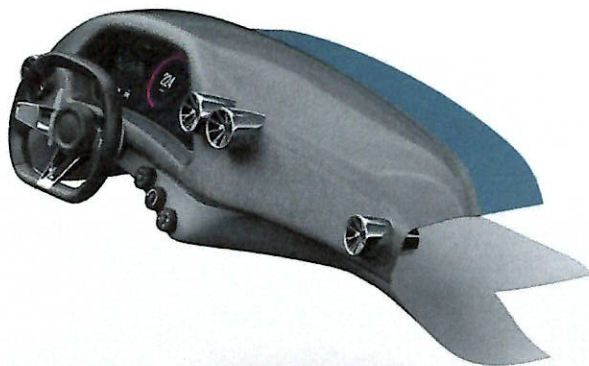


Fig. 7 Concept 2

The advantage of such a model is the decrease of the molds complexity for the main part and a simplification of the maintenance operations. There are more molds required to make the two extra pieces though. The first piece comes under the windscreen; it will hold the dashboard in place and may have a role in demisting the windshield. The second piece comes under the dashboard; it supports it from beneath and has an aesthetical and functional role in delimiting the space for the driver's and passenger's legs. If it's necessary control elements can be fitted with control buttons and nos.

3.3 Concept 3

This concept involve the mounting of two pieces on top of each other, so the lower part acts as a support, it can be fitted with ventilation holes and various controls and control elements, nob. The upper part may also contain ventilation holes and on-board instruments.

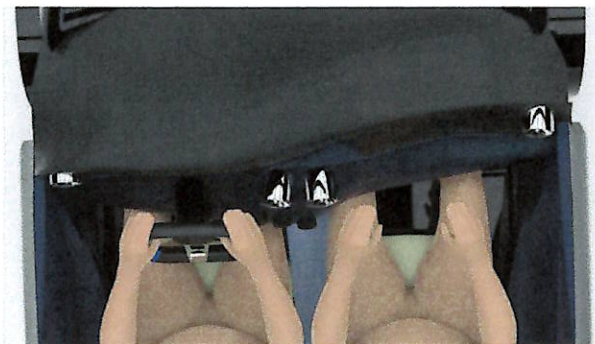


Fig.8 Concept 3

By removing the upper part of the dashboard assembly during maintenance operations, the mechanics have direct access to the components that normally are inaccessible in the case of a classic dashboard without removing it. In the case of Concept 3, two molds would be needed to manufacture it, but the resulting shapes and the design lines could be more complex than a one-piece dashboards'.

4. MANUFCATURING TECHNOLOGY

In the embodiment shown in Figure 10 for the manufacturing of the dashboard it is possible to use a composite material reinforced with glass fiber or carbon fiber / epoxy matrices. The use of these materials leads to the reduction of the components' mass, as an essential condition to increase the autonomy of the electric vehicle. The chosen layer architecture is [+45/0-90/]. Carbon fiber layers are Twill fabric type 240g/m2.

For a variant where the product requires enhanced rigidity characteristics, a sandwich structure is proposed with two layers of 240g / m² Twill carbon fiber fabric as outer layers. Layer configuration [+45/0-90/]. Between the two layers of carbon fiber, the core of the sandwich structure will be made of 1 mm Coremat or 2 mm of Rohacel.

In the area where it is possible to insert the airbag, the structure will be made up of two layers of 90g/m² plain carbon fiber fabric ad +45 degrees. This will be available only on the outside of the dashboard. In the middle will be kept the 2 mm thick Rohacel structure. The structure will not be doubled by another wall inwards. This will allow a slight damage to the outside surface to allow the impact cushion to come out in case of an impact, when the charge of the airbag detonates.

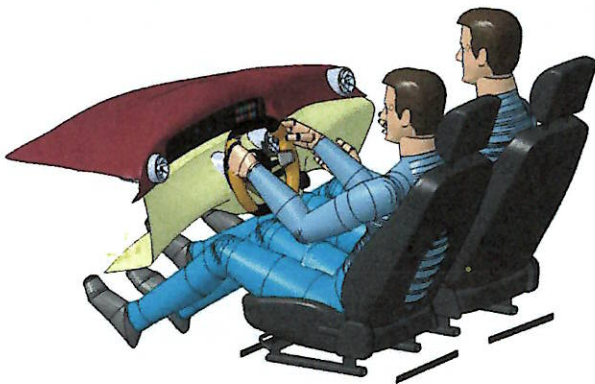


Fig. 9 The two-piece dashboard

The outer shape of the dashboard for the chosen configuration allows the components to be made in two separate molds. The upper part, marked 1, in Figure 10 can be manufactured in a concave mold. This does not require an additional separation plane. It can be easily extracted from the mold, and the fabric can be applied to the entire surface without the need for cuts or cut-outs. These could optically influence the outer design of the piece. Cut-outs for the vent holes will then be cut in the pre-set positions. From the molds' point of view regarding the manufacturing, the proposed solution is to use epoxy blocks processed on CNC centers as material. This is the fastest solution for making composite prototype parts and offers a good surface finish in a relative short time.

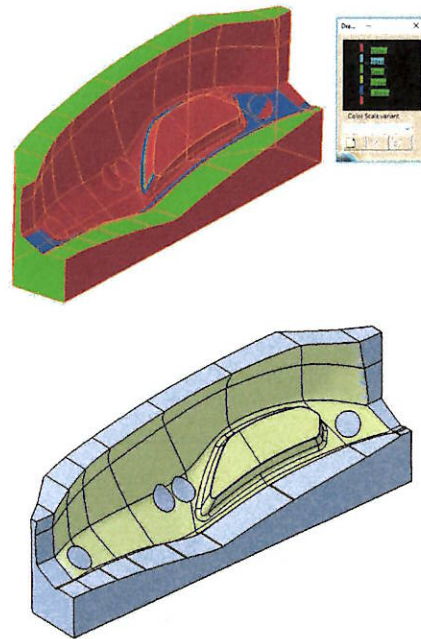


Fig. 10 Concave moulds for the dashboard

The lower part of the dashboard, marked 2 in Figure 10, is made of the same material and can be made in a separate cavity mold. Thanks to its generous shape, it allows to be produced from one piece. The fastening of the two parts is done with screws on the inside, which allows a rigid assembly. A gasket is proposed to be used between the two components to reduce the noise occurred in the joint area of the rigid components while the vehicle is in motion.

The modular design of the dashboard, in addition to adopting a simpler solution for the composite parts, offers the possibility of a high degree of interchangeability of components. This solution allows to change the upper part and use another design. When using right-hand drive vehicles, only the upper part of the dashboard must be changed. Often, interventions for repairs occur in the interior area of the dashboard. Using this concept, by removing one of the parts the workers have easier access to the interior elements of the dashboard.

In the mounting areas of the dashboard onto the chassis, metal plates (in which the holes will be applied) will be integrated between the layers of composite materials. Metal inserts are designed to prevent damage of the composite material (with anisotropic properties), the

mechanical stress being absorbed by a homogeneous material (metal).

5. CONCLUSION

Making a composite dashboard is a feasible solution, which can be made in several design variants. In this paper are presented three versions of a dashboard, chosen so that in technological and functional aspect to fulfil all the functions of a classic dashboard. The major advantage of a dashboard made of composite materials is its weight, which is easier than a classic one with at least 60%. A possible problem is the overheating of the dashboard in the summer, when the car is exposed to direct sunlight and the dashboard if it's not covered in any other type of materials similar to those used on a classic dashboard. The cost of manufacturing of a composite dashboard is lower than in the case of a classic one, but the operation cannot be automated. The finishes used may be the same as those used for a classic dashboard. Reduced weight is an advantage for electric cars where the cars' autonomy is directly influenced by their weight.

6. ACKNOWLEDGMENTS

This work was supported by a grant of the Romanian National Authority for Scientific Research and Innovation, CNCS/CCCDI-UEFISCDI, project number PN-III-P2-2.1-96BG-2016-0210, within PNCDI III.¶ (12pt)

7. REFERENCES

1. Shanghai, V. *Composite materials on Tesla Concept dashboard*. 2017 [cited 2018 June]; Available from: <https://medium.com/inspiration-supply/car-dashboard-ui-ux-concepts-d135959d963f>.
2. Nevozhai, D. *BMW Car Dashboard Design*, [cited 2018 June]; Available from: <https://www.behance.net/gallery/12354511/BMW-Car-Dashboard-Design>.
3. Kim, S., et al., *Usability of Car Dashboard Displays for Elder Drivers*.

4. Zhang, W.H. and Destech, *Design of Large Injection Mold for Car Dashboard*. International Conference on Information Technology and Industrial Automation. 2015, Lancaster: Destech Publications, Inc. 24-31.
5. Mantovani, S., et al., *Influence of manufacturing constraints on the topology optimization of an automotive dashboard*, in 27th International Conference on Flexible Automation and Intelligent Manufacturing, Faim2017, M. Pellicciari and M. Peruzzini, Editors. 2017, Elsevier Science Bv: Amsterdam. p. 1700-1708.
6. Cebi, S. and C. Kahraman, *Design evaluation model for display designs of automobiles*. Journal of Intelligent & Fuzzy Systems, 2014. 26(2): p. 961-973.
7. Kessler, D. and C. Grabowski, *Volumetric, dashboard-mounted augmented display*, in International Optical Design Conference 2017, P.P. Clark, et al., Editors. 2017, Spie-Int Soc Optical Engineering: Bellingham.
8. Rosli, U., et al., *Problems Evaluation for TRIZ Method using AHP: Case Study on Car's Dashboard Improvement Design Concepts*, in Advances in Mechanical and Manufacturing Engineering, Z.A. Zulkefli, et al., Editors. 2014, Trans Tech Publications Ltd: Stafa-Zurich. p. 89-93.
9. www.agency-power.com. Agency Power Carbon Fiber Dash Polaris RZR XP 1000. 2018 [cited 2018 June]; Available from: <https://www.agency-power.com/shop/agency-power-carbon-fiber-dash-polaris-rzr-xp-1000-turbo-14-16/?v=f5b15f58caba>.

Utilizarea materialelor composite pentru proiectarea bordului unei masini electrice

Rezumat: Lucrarea prezinta un panou de bord realizat integral din material composite, proiectat pentru o masina electrica cu doi pasageri. Sunt prezentate si analizate posibilitatile de realizare a panoului de bord, precum si un model optimizat al bordului care poate fi realizat in intregime din materiale composite.

Sergiu SOLCAN, Technical University of Cluj-Napoca, Design Engineering and Robotics, Bd. Muncii 103-105, Romania, solcansergiu@yahoo.com

Calin NEAMTU, Technical University of Cluj-Napoca, Design Engineering and Robotics, Bd. Muncii 103-105, Romania, calin.neamtu@muri.utcluj.ro

Paul BERE, Technical University of Cluj-Napoca, Manufacturing Engineering, Bd. Muncii 103-105, Romania, paul.ber@tcm.utcluj.ro

Rares GHINEA, Technical University of Cluj-Napoca, Design Engineering and Robotics, Bd. Muncii 103-105, Romania, rares.ghinea@muri.utcluj.ro

Raul ROZSOS, Technical University of Cluj-Napoca, Design Engineering and Robotics, Bd. Muncii 103-105, Romania, rozsos_raul.silviu@yahoo.com

Attila PAPP, Magic Engineering, Mugurului, Nr. 4, Ap. 1, OP 2, CP 131, 500301 – Brasov, Romania, attila.papp@magic-engineering.ro





TECHNICAL UNIVERSITY OF CLUJ-NAPOCA

ACTA TECHNICA NAPOCENSIS

Series: Applied Mathematics, Mechanics, and Engineering
Vol. 64, Issue I, March, 2021

DESIGN AND ERGONOMIC ANALYSIS OF CAR DOORS MADE FROM COMPOSITE MATERIALS

Sergiu SOLCAN, Ștefan BODI, Radu COMES, Raul-Silviu ROZSOS, Călin NEAMȚU,
Cătălin COCEAN

Abstract: This paper presents the design of an interior panel of a door for a small electric car intended for urban traffic. The design incorporates a display that replaces the mirror, the ambient light in the storage compartment is activated automatically by a proximity sensor, and the whole panel can be made entirely out of carbon fiber or in combination with plastic parts/components.

Key words: AHP, carbon fiber, interior car design.

1. INTRODUCTION

The composite materials used in the construction of structures in various fields (automotive, naval, civil, aerospace) are becoming more and more effective in providing good mechanical properties, temperature resistance, abrasion and cracking resistance, high resilience, stability to chemical agents, etc. [1]-[4]. Carbon fiber reinforced plastics (CFRP) are one of the most used composite material because of their excellent properties [5]-[8], such as light weight mass, high durability, high modulus, good fatigue and corrosion resistance [9]-[11].

Car design has evolved from simple shapes to complex ones (Fig. 1) due to the growing needs of end users and technological progress. Today, in the dashboards and door panels, there are sensors and displays that increase the comfort of end users. For example, the rearview mirrors are replaced by cameras and displays, mounted on the door or on the dashboard, there are proximity sensors that turn on ambient lights in the door when the user inserts his hand in the storage compartment, fingerprint sensors for opening and closing the vehicle or exterior lights that illuminate the area when exiting the vehicle or displays various patterns, such as the car logo [7], [12]-[15].

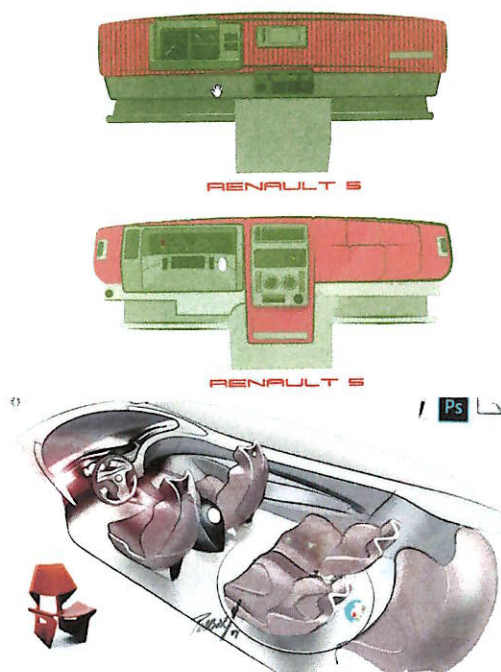


Fig. 1 Design concept evolution [1]

2. DESIGNING THE DOOR PANEL FOR AN ELECTRIC CAR

The aim of the paper is to present the way in which the design of the interior panel of a door from a light electric vehicle (indicated in Fig. 2), intended for the urban environment, has unfolded. The main constraint was the use of carbon fiber composite material in the

manufacturing of the interior side of the door (Fig. 3).



Fig. 4 Design concept of electric vehicle

The design has evolved from a simple one-piece door panel to one that has storage space, space for the audio system components and a built-in screen for the electronic system that replaces the mirror.

The main instruments used in the development of the concept were the Analytical Hierarchy Process (AHP) analysis and ergonomic analysis of the occupant’s position for determining the critical requirements that an end user might have when seated inside the vehicle.

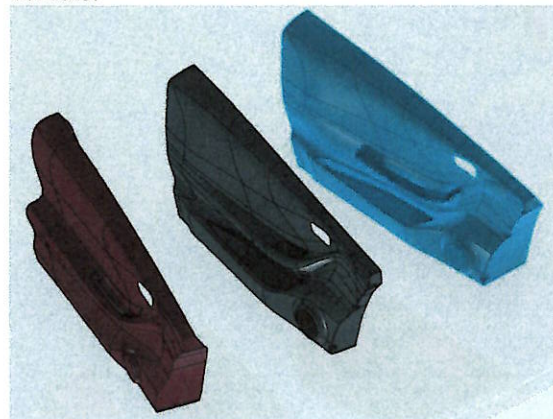


Fig. 5 The design development of the interior part of the door.

Item Number	1	2	3	4	5	6	7	8	9	10
1 Integrated controls for windows, mirrors, lock / unlock doors	1.00	6.00	7.00	6.00	7.00	9.00	5.00	6.00	5.00	9.00
2 Extendable trim panel tray with proximity / motion sensor and integrated light	0.17	1.00	5.00	0.50	4.00	7.00	4.00	5.00	4.00	7.00
3 Ergonomic grip for door handle and door release knob	0.14	0.20	1.00	0.25	0.20	2.00	0.17	0.50	0.33	2.00
4 Reliable inside door handle	0.17	2.00	4.00	1.00	4.00	7.00	4.00	3.00	7.00	6.00
5 Integrated bottle/cup holder	0.14	0.25	5.00	0.25	1.00	4.00	2.00	5.00	5.00	3.00
6 Warn light reflective strip / reflector dots	0.11	0.14	0.50	0.14	0.25	1.00	0.17	0.50	0.20	0.17
7 Integrated left arm rest	0.20	0.25	6.00	0.25	0.50	6.00	1.00	6.00	4.00	7.00
8 Easy to clean / antiseptic materials	0.17	0.20	2.00	0.33	0.20	2.00	0.17	1.00	0.50	2.00
9 Customizable finishing materials for panel trim	0.20	0.25	3.00	0.14	0.20	5.00	0.25	2.00	1.00	2.00
10 Use of highly insulating materials	0.11	0.14	0.50	0.17	0.33	6.00	0.14	0.50	0.50	1.00
Sum	2.41	10.44	34.00	9.04	17.68	49.00	16.89	29.50	27.53	39.17

Fig. 6 Pairwise comparison matrix

The AHP method was preceded by a classic brainstorming session, through which a team of 8 engineers (including the authors) determined some critical requirements regarding the car door panel. The obtained set of 10 requirements was inputted into an AHP analysis with the purpose of ranking these criteria, similar as in [16] and [18]. The analysis unfolded through three main stages.

In the first stage, an NxN matrix was devised, and all the criteria were compared to each other

in a pairwise fashion. Thus, the matrix was completed using the Saaty scale of comparison: if a row item is more important than a column item a whole number is used (n), else a fractional number (1/n) is inserted; in both cases “n” represents the end user’s assessment of the importance ratio between the two compared items. Based on the values from the matrix the sum for each column was calculated (see Fig. 6).

The values from the “standardized matrix” were obtained by dividing the corresponding

number from the “pairwise comparison matrix” with the sum obtained for each column (e.g. the value from row 3, column 1 from the standardized matrix is equal to the value from row 3, column 1 from the pairwise comparison

matrix over the sum of the first column – $0.14/2.41 \approx 0.06$). Next, by calculating the average on each row, the weight of each requirement is obtained (see Fig. 5).

	1	2	3	4	5	6	7	8	9	10	Weight
1 Integrated controls for windows, mirrors, lock / unlock doors	0.42	0.57	0.21	0.66	0.40	0.18	0.30	0.20	0.18	0.23	33.5%
2 Extendable trim panel tray with proximity / motion sensor and integrated light	0.07	0.10	0.15	0.06	0.23	0.14	0.24	0.17	0.15	0.18	14.7%
3 Ergonomic grip for door handle and door release knob	0.06	0.02	0.03	0.03	0.01	0.04	0.01	0.02	0.01	0.05	2.8%
4 Reliable inside door handle	0.07	0.19	0.12	0.11	0.23	0.14	0.24	0.10	0.25	0.15	16.0%
5 Integrated bottle/cup holder	0.06	0.02	0.15	0.03	0.06	0.08	0.12	0.17	0.18	0.08	9.4%
6 Warn light reflective strip / reflector dots	0.05	0.01	0.01	0.02	0.01	0.02	0.01	0.02	0.01	0.00	1.6%
7 Integrated left arm rest	0.08	0.02	0.18	0.03	0.03	0.12	0.06	0.20	0.15	0.18	10.5%
8 Easy to clean / antiseptic materials	0.07	0.02	0.06	0.04	0.01	0.04	0.01	0.03	0.02	0.05	3.5%
9 Customizable finishing materials for panel trim	0.08	0.02	0.09	0.02	0.01	0.10	0.01	0.07	0.04	0.05	4.9%
10 Use of highly insulating materials	0.05	0.01	0.01	0.02	0.02	0.12	0.01	0.02	0.02	0.03	3.0%

Fig. 7 Standardized matrix

Finally, for making sure that the “pairwise comparison matrix” was filled out as correctly as possible and to determine how consistent the judgements have been when completing the AHP pairwise comparison matrix, the “consistency ratio” (CR) is also calculated. Normally, as Thomas L. Saaty suggests (the inventor of the AHP mathematical model for decision support) to be tolerable, the CR should be between 0 and 0.1, in this case it’s CR = 0.08 [17].

Based on the hierarchy of identified requirements, a preliminary 3D model was created (Fig. 8), which was then used in the ergonomics analysis using CATIA V5-6 software.



Fig. 8 Preliminary 3D model

The initial set-up includes the parameters from Table 1 and Fig. 7.

Table 1 Ergonomics parameters for driver's seat

Param.	Value	Param.	Value
L31-1	1200mm	A40-1	25deg
W20-1	-380mm	L11	440mm
H30-1	200mm	W7	-380mm
A19	0deg	H17	580mm
TL2	50mm	W9	380mm
TL18	200	A18	20deg
A27-1	20deg	SWDiam.	30mm

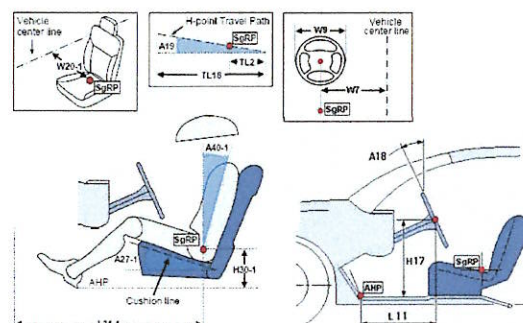


Fig. 9 Driver's seat parameter illustration

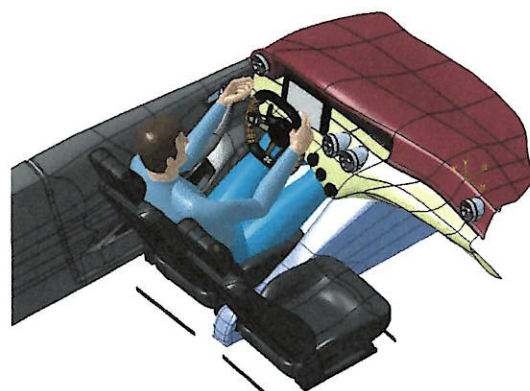


Fig. 10 Initial set-up

3. RESULTS

For the design of the armrest and the handle (Fig. 11) the final angle at which the design was made is 50 degrees for the elbow joint (minimum value is 0 degrees and maximum is 140 degrees) and 8 degrees in horizontal plane for the shoulder joint. In order to verify the way in which a display can be integrated into the design to replace the rear-view mirror, the "Vision" function was employed in CATIA (Fig. 13), through which the field of vision of the driver can be determined and analyzed, when the driver is seated in a normal driving position. Thus, the position of the mirror(s) relative to the seats and steering wheel can be determined, so that the mirror or the display that replaces it is permanently in the driver's field of vision.

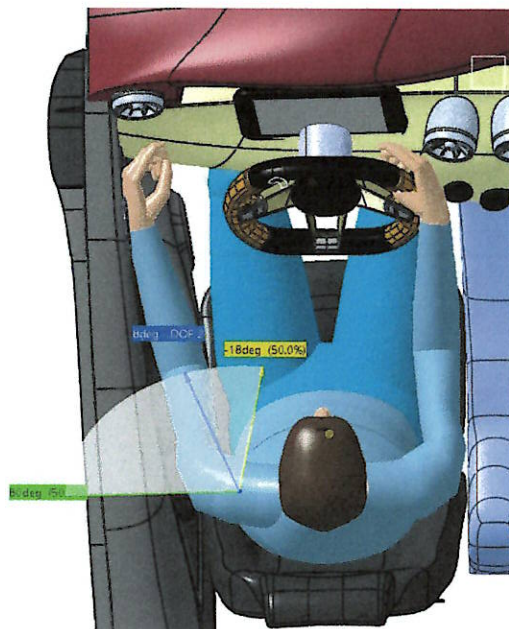
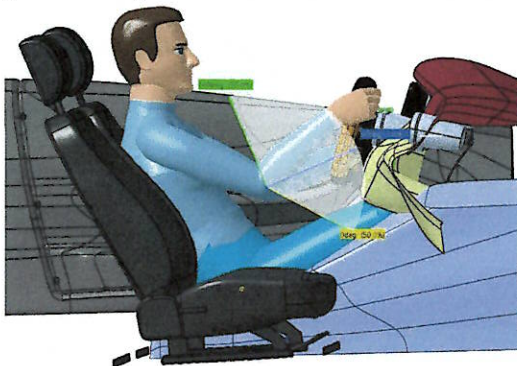


Fig. 11 Vertical and horizontal angle for the elbow and shoulder joint

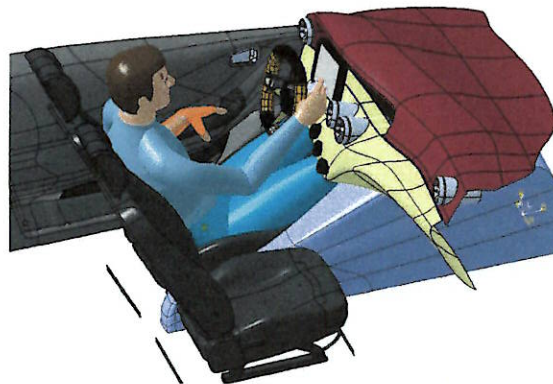


Fig. 12 Position of the driver when the door is closed

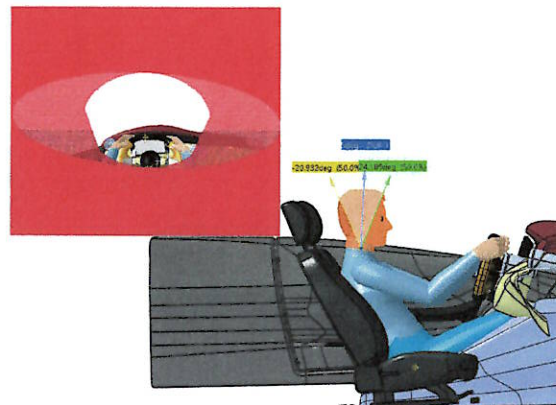


Fig. 13 Visual field



Fig. 14 Model 3D final

The final version of the door (Fig. 14) can include a detachable plastic handle or an integrated carbon fiber handle, a light source (LED) in the storage compartment controlled by the proximity sensor and a display that replaces the rear-view mirror.

The first version of car door was entirely fabricated using composite materials: the first layer is CFRP prepreg type GG245TSE-DT121H-42 and the enforcement material is the Twill 2X2 fabric, 240g/mp, 3K HR threads; the second and third layer is prepreg GG430TSE-DT121H-42 and the enforcement material is the Twill 2X2 fabric, 430g/mp, 12K HR threads. The configuration of the layers is $[0/90/\pm 45/0/90]$. A reinforced area also is included (the green area from Fig. 15), to which a prepreg type GG245TSE-DT121H-42 material is added, in two layers, with the $[0/90/\pm 45]$ configuration. In this area the door flap and the opening/closing mechanism is added, alongside the door handle, which can be pulled or pushed to close or to open the door.

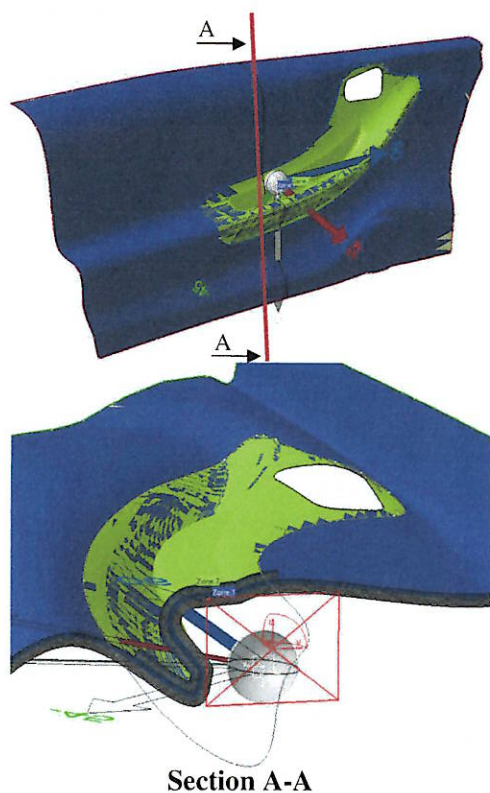


Fig. 15 Arrangement of the layers of material for the first version of the door

The modeling of the composite material was completed in CATIA V5 (see Fig. 15), the obtained results are presented in Table 2.

Table 2. Surface area and mass for the 1st version of the door

	Area	Mass
Zone 1	6.14 m ²	1.939 kg
Zone 2	0.61 m ²	0.254 kg
Total	6.75 m ²	2.193 kg

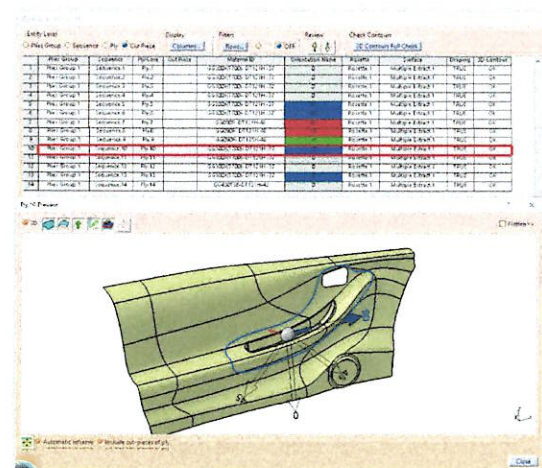


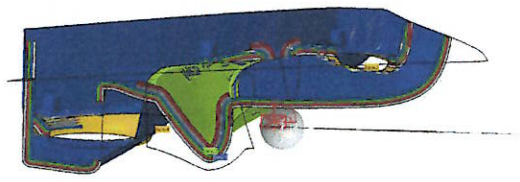
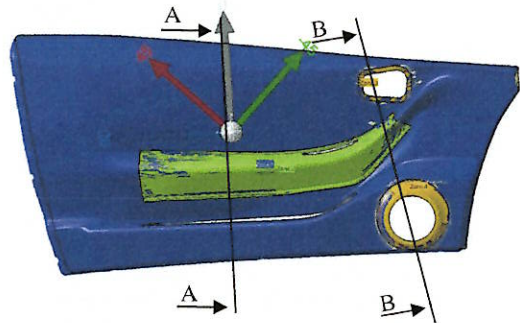
Fig. 16 Stacking management for the composite material layers

The second version of the door is made of the same composite material as the first version with the mention that here there are three reinforced areas. The first area is that of the handle, the second that of the opening flap and the third area in which the car audio system speaker is mounted. In these three areas prepreg type GG245TSE-DT121H-42 is added, in two layers, in the $[0/90/\pm 45]$ configuration.

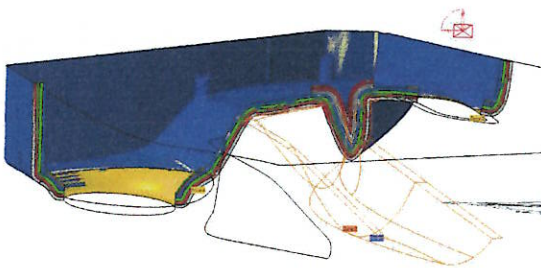
In Fig. 17 are presented the three areas, as well as two sections through these areas in which it is possible to observe the way in which the material layers are arranged. As it can be seen in Table 3, the material quantity is lesser and implicitly the weight is lighter, too, which is due to the fact that the reinforced areas have a smaller unfolded surface than in the first case.

Table 3. Surface area and mass for the 2nd version of the door

	Area	Mass
Zone 1	3.55 m ²	1.60 kg
Zone 2	0.48 m ²	0.135 kg
Zone 3	0.008 m ²	0.002 kg
Zone 4	0.034m ²	0.007 kg
Total	4.72 m ²	1.737 kg



Section A-A



Section B-B

Fig. 17 Arrangement of layers of the composite materials, second version

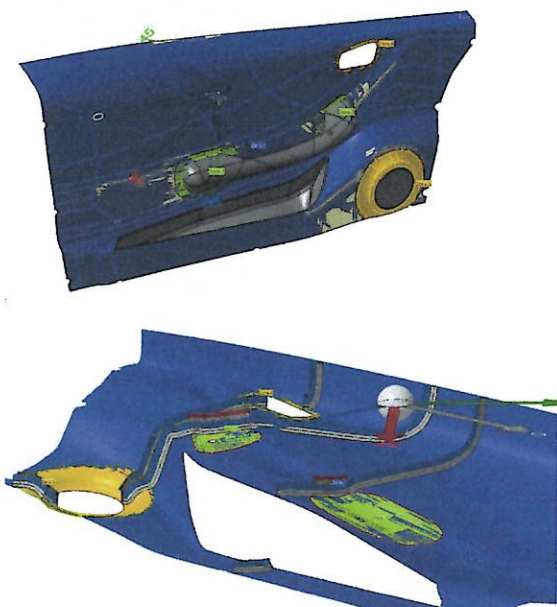


Fig. 18 Arrangement of layers of the composite materials, third version

In the third version of the interior door panel, the handle is made of plastic and is fixed to a similar panel, as in the case of classic doors with a threaded assembly. Consequently, only the areas where this type of assembly is made have been reinforced. There are two other reinforced areas at the opening flap and in the area where the audio system speaker is mounted.

Table 4 shows the material requirements and the final weight of the door panel.

Table 4. Surface area and mass for the 3rd version of the door

	Area	Mass
Zone 1	2.45 m ²	1.10 kg
Zone 2	0.09 m ²	0.25 kg
Zone 3	0.042 m ²	0.012 kg
Zone 4	0.008m ²	0.002 kg
Zone 5	0.046 m ²	0.009 kg
Total	2.636 m ²	1.373 kg

4. CONCLUSIONS

The validation of the 3D model was completed using interactive virtual reality environments (Fig. 19), in which the developer/designer was fully immersed and interacted with the 3D model of the door panel, as well as the dashboard.



Fig. 19 The validation process in the interactive virtual reality environments

Using the Composite Design module from CATIA V5, the composite material from which the door panel can be manufactured was modeled for each constructive solution (variants/versions). The optimal version in terms of material consumption and weight is the is the

third version of the door, in which the reinforced areas are the smallest, thus the material consumption is lesser, and the weight is lower.

5. REFERENCES

- [1] Zinno, A.; Fusco, E.; Prota, A.; Manfredi G.; Multiscale approach for the design of composite sandwich structures for train application, *Composite Structures*, Vol. 92, Iss. 9, pp. 2208–2219, 2010, DOI:10.1016/j.compstruct.2009.08.044
- [2] Sabău E.; Bălc N.; Bere P.; Mechanical characteristics of composite materials obtained by different technologies, *Academic Journal of Manufacturing Engineering – AJME*, Vol. 9, Iss. 4, 2011, ISSN 1583-7904, ISSUE 4/ 2011
- [3] Belouettar, S.; Abbadi, A.; Azari, Z.; Belouettar, R.; Freres, P.; Experimental investigation of static and fatigue behaviour of composites honeycomb materials using four-point bending tests. *Composite Structures*, Vol. 87, Iss. 3, pp. 265-273, 2009, DOI: 10.1016/j.compstruct.2008.01.015
- [4] Abbadi, A.; Koutsawa, Y.; Carmasol, A.; Belouettar, S.; Azari, Z.; Experimental and numerical characterization of honeycomb sandwich composite panels, *Simulation Modelling Practice and Theory*, Vol. 17, Iss. 10, pp. 1533–1547, 2009, DOI:10.1016/j.simpat.2009.05.008
- [5] Ceclan V.; Bere P.; Borzan M.; Development of environmental technology for carbon fibre reinforced materials recycling, *Materials Science*, Vol. 50, Iss. 2, 2013, ISSN 0025-5289
- [6] He, M.; Hu, W.; A study on composite honeycomb sandwich panel structure, *Materials and Design*, Vol. 29, Iss. 3, pp. 709–713, 2008, DOI:10.1016/j.matdes.2007.03.003
- [7] Liu, Q.; Lin, Y.; Zong, Z.; Sun, G.; Li, Q.; Lightweight design of carbon twill weave fabric composite body structure for electric vehicle, *Composite Structures* Vol. 97, pp. 231-238, 2013, DOI:10.1016/j.compstruct.2012.09.052
- [8] Bere, P.; Krolczyk, J.B.; Determination of mechanical properties of carbon/epoxy plates by tensile stress test, *E3S Web of Conferences* 19 (International Conf. Energy, Environment and Material Systems – EEMS 2017), 03018, 2017, DOI:10.1051/e3sconf/20171903018
- [9] ASTM D3039/D 3039M-00, Standard Test Method for Tensile Properties of Polymer Matrix Composite Materials
- [10] ASTM D 3518/D 3518M – 94, Standard Test Method for In-Plane Shear Response of Polymer Matrix Composite Materials by Tensile Test of a $\pm 45^\circ$ Laminate
- [11] ASTM D 7264/D 7264M – 07, Standard Test Method for Flexural Properties of Polymer Matrix Composite Materials
- [12] Bere, P.; Neamtu C.; Methodology for evaluate the form deviations for formula one nose car, *Central European Journal of Engineering*, Vol. 4, Iss. 2, 2014, ISSN: 1896-1541, DOI:10.2478/s13531-013-0158-x
- [13] Mantovani S.; Campo, G.A.; Ferrari, A.; Cavazzuti, M.; Optimization methodology for automotive chassis design by truss frame: A preliminary investigation using the lattice approach, *25th ISPE International Conference on Transdisciplinary Engineering, Advances in Transdisciplinary Engineering* Vol. 7, Iss. 3, pp.984-992, 2018, DOI:10.3233/978-1-61499-898-3-984
- [14] Mantovani, S.; Presti, I.L.; Cavazzoni, L.; Baldini, A.; Influence of manufacturing constraints on the topology optimization of an automotive dashboard, *Procedia Manufacturing*, Vol. 11, pp. 1700-1708, DOI:10.1016/j.promfg.2017.07.296, 2017
- [15] Presti, I.L.; Cavazzoni, L.; Calacci, F.; Mantovani, S.; Optimization methodology for an automotive cross-member in composite material, *Key Engineering Materials* Vol. 754, Trans Tech Publications Ltd, pp.291-294, 2017, DOI:10.4028/www.scientific.net/KEM.754.291
- [16] Dragomir, D.; Cicală, I.; Dragomir, I.; Bodi, S.; Proposed instrument for aiding in the implementation of a Social Responsibility Management System, *Quality-Access to Success*, Vol. 13, Iss. 5, pp. 123-126, 2012
- [17] Dragomir, M.; Iamandi, O.; Bodi, S.; Designing a roadmap for performance indicators in integrated Management Systems, *Managerial Challenges of the Contemporary Society*, Vol. 5, 2013, pp. 91-95, ISSN 2069-4229

Rozs

- [18] Rozsos, R.S.; Buna, Z.; Bodi, S.; Comes, R.; Tompa, V.; Design and development of a linear DELTA 3D printer, Acta Technica Napocensis – Series: Applied Mathematics, Mechanics, and Engineering, Vol. 63, Iss. 2, pp. 185-190, 2020.

Acknowledgement

This work was supported by the project “Advanced technologies for intelligent urban electric vehicles”- URBIVEL – Contract no.11/01.09.2016, project co-funded from the European Regional Development Fund through the Competitiveness Operational Program 2014-2020

PROIECTAREA ȘI ANALIZA ERGONOMICĂ A UNUI PANOU INTERIOR DE UȘĂ PENTRU UN AUTOMOBIL FABRICAT DIN MATERIALE COMPOZITE

Abstract: *Lucrarea prezintă designul unui panou interior al unei uși pentru o mașină electrică de mici dimensiuni destinată traficului urban. Designul încorporează un display care înlocuiește oglinda, lumină ambientală în compartimentul de depozitare, activată automat printr-un senzor de prezență și care poate fi fabricat integral din carbon sau în combinație cu piese din plastic.*

Sergiu SOLCAN, Ph.D. candidate, Eng., Department of Design Engineering and Robotics, Technical University of Cluj-Napoca, solcansergiu@yahoo.com, 103-105 Muncii Blvd., 400641 Cluj-Napoca, Cluj county, Romania

Ștefan BODI, Ph.D., Eng., Lecturer at the Department of Design Engineering and Robotics, Technical University of Cluj-Napoca, stefan.bodi@muri.utcluj.ro, 103-105 Muncii Blvd., 400641 Cluj-Napoca, Cluj county, Romania

Radu COMES, Ph.D., Eng., Lecturer at the Department of Design Engineering and Robotics, Technical University of Cluj-Napoca, radu.comes@muri.utcluj.ro, 103-105 Muncii Blvd., 400641 Cluj-Napoca, Cluj county, Romania

Raul-Silviu ROZSOS, Ph.D. candidate, Eng., Department of Design Engineering and Robotics, Technical University of Cluj-Napoca, Romania, raul.rozsos@muri.utcluj.ro, 103-105 Muncii Blvd., 400641 Cluj-Napoca, Cluj county, Romania

Călin NEAMȚU Ph.D., Eng., Professor at the Department of Design Engineering and Robotics, Technical University of Cluj-Napoca, calin.neamtu@muri.utcluj.ro, 103-105 Muncii Blvd., 400641 Cluj-Napoca, Cluj county, Romania

Cătălin COCEAN, Eng., Belco-Avia S.R.L., 423 Cruci St., 427120 Livezile, Bistrița-Năsăud county, Romania



TECHNICAL UNIVERSITY OF CLUJ-NAPOCA

ACTA TECHNICA NAPOCENSIS

Series: Applied Mathematics, Mechanics, and Engineering
Vol. 62, Issue IV, November, 2019

USING IMAGE PROCESSING TO AUTHENTICATE ARTWORK (II)

Rareş GHINEA, Vasile TOMPA, Zsolt BUNA, Raul ROZSOS, Daniela POPESCU,
Ciprian FIREA

Abstract: The paper proposes to validate an algorithm for the automatic identification of 2D elements by image processing based on Cross Correlation. The algorithm uses a modified version of Cross Correlation that allows the identification of a template even if they change its position and orientation in an image. The validation of the mathematical model was carried out in Matlab on a series of standard photographs. Having the mathematical model validated, the proposed algorithm has been used in the authentication of works of art.

Keywords: artwork, image processing, cross-correlation, pattern detection.

1. INTRODUCTION

There is an increasing trend and interest for art institutions world-wide to digitize their cultural repository [1-3], not only to increase their audience, but also to further investigate, or submit digitized artwork to all kinds of analyses. For this demarche image processing is used, which facilitates investigations such as image emotion detection [4], feature and pattern recognition [5, 6] or even artwork authentication [7][6]. All these are challenging tasks which often are completed by calculating the correlation degree between a reference and an examined image, thus providing a clear indication of affinity or divergence between the two. This process is referred to as cross-correlation, an algorithm which evolved significantly over time, from accuracy analysis [8] to fast normalized cross correlation [9-11] and pattern detection using normalized neural networks [6].

1.1. Main objectives

The project's main objectives are:

- Development of a specific methodology for data and image acquisition, management and processing, dedicated for 2D artwork artifacts;
- Adaptation and integration of existing hardware and software instruments to provide maximum efficiency for the automated feature recognition;
- Definition, implementation and optimization of a dedicated database, which would assist the academic communities in their future studies and research work.

2. PROPOSED ALGORITHM

2.1 Matching Templates using Cross – Correlation

The term cross-correlation which refers to the correlation between two signals is viewed as a standard approach when trying to detect features [12, 13]. Literature presentations of correlation describe the convolution theorem. They also describe the attendant possibility of computing correlation efficiently in the domain of frequency analysis using the fast Fourier transform. Unfortunately, the correlation coefficient, which is the normalized form of correlation that is preferred in template

Rozsos

matching, does not have simple and efficient expression in the frequency domain [14]. This is the reason why normalized cross – correlation has been computed in the spatial domain [15]. Because of the high computational cost of spatial domain convolution, several fast but inexact spatial domain matching methods were developed [14]. The algorithm [16] used in order to obtain the normalized cross correlation will be presented using the equations represented below.

The use of cross-correlation for template matching is motivated by the distance measure (squared Euclidean distance)

$$d_{f,t}^2(u, v) = \sum_{x,y} [f(x, y) - t(x - u, y - v)]^2 \quad (1)$$

where f is the image and the sum is over x, y under the window containing the feature t positioned at u, v . In the expansion of d^2 :

$$d_{f,t}^2(u, v) = \sum_{x,y} [f^2(x, y) - 2f(x, y)t(x - u, y - v) + t^2(x - u, y - v)] \quad (2)$$

the term $\sum t^2(x - u, y - v)$ is constant.

If the term $\sum f^2(x, y)$ is approximately constant, then the remaining cross – correlation term :

$$c(u, v) = \sum_{x,y} f(x, y)t(x - u, y - v) \quad (3)$$

is a measure of the similarity between the image and the feature.

There are several disadvantages for using (3) for template matching:

- If the image energy $\sum f^2(x, y)$ varies with position, matching with (3) can fail. For example, the correlation between the feature and an exactly matching region in the image may be less than the correlation between the feature and a bright spot.
- The range of $c(u, v)$ is dependent on the size of the feature

- Equation (3) is not invariant to changes in image amplitude such as those caused by changing lightning conditions across the image sequence.

The issue that needs to be addressed is the identification of artwork using an array of graphical elements that define the work style of each studied painter. In the first stage of algorithm development there will be used images that contain average items (screws, coins, etc.) in different positions or alignment. One of the identified issues was the variation of the light in the images if they were not taken in a studio using the same light conditions. (Fig. 1).

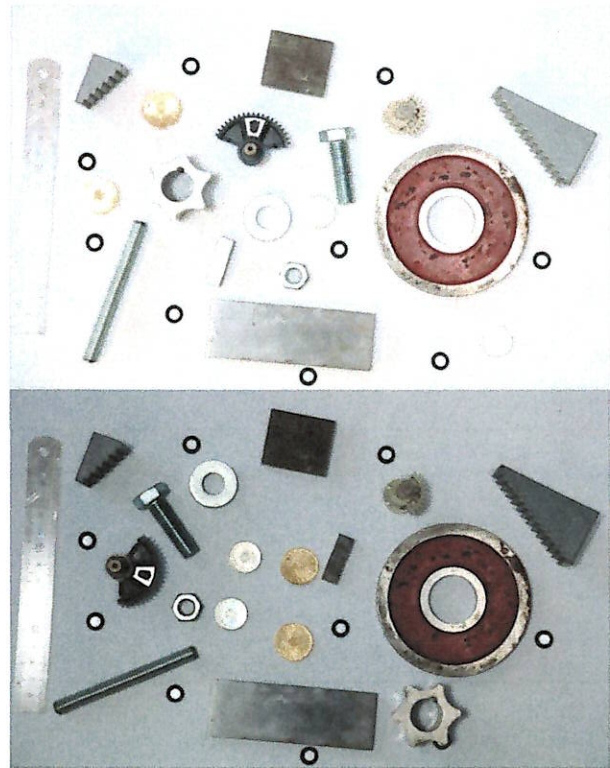


Fig. 1 Images used for algorithm validation

For image-processing applications in which the brightness of the image and template can vary due to lighting and exposure conditions, the images can be first normalized. This is typically done at every step by subtracting the mean and dividing by the standard deviation.

That is, the cross-correlation of a template, $t(x, y)$ with a sub image $f(x, y)$ is :

$$c(u, v) = \frac{1}{n} \sum_{x,y} \frac{1}{\sigma_f \sigma_t} (f(x, y) - \mu_f)(t(x, y) - \mu_t) \quad (4)$$

where n is the number of pixels in $t(x,y)$ and $f(x,y)$, μ_f is the average of f and σ_f is standard deviation of f .

After eliminating the effects of brightness and contrast of the image, the next problem to be solved is the orientation $t(x,y)$ (ROI) with respect to $f(x,y)$.



Fig. 2 ROI relative positions

To solve the orientation problem, a rotation matrix between these two images $t(x,y)$ and $f(x,y)$ must be determined. A loop is created in which the image $t(x,y)$ is incrementally rotated clockwise and incrementally translated to the image $f(x,y)$. For each position it is determined the correlation factor that allows quantitative assessment of the degree of matching between ROI (Region Of Interest) (t) and the image in which it is searched (f).

$$\gamma = \frac{\sum_{x,y} (f(x,y) - \bar{f}_{u,v})(t(x-u,y-v) - \bar{t})}{\sqrt{\sum_{x,y} (f(x,y) - \bar{f}_{u,v})^2 \sum_{x,y} (t(x-u,y-v) - \bar{t})^2}} \quad (5)$$

3. ALGORITHM IMPLEMENTATION

3.1 Image acquisition

In the validation stage the image acquisition has been done in the laboratory under controlled conditions to minimize the influences due to the variation of light and contrast. A composition of items that contains several similar objects has been created, several photographs were taken in which the positions of three objects remained constant and the rest were modified so that it could be tested to identify similar elements in

different positions. In Fig. 3 presents the images that have been used and Fig. 4 highlight the results.

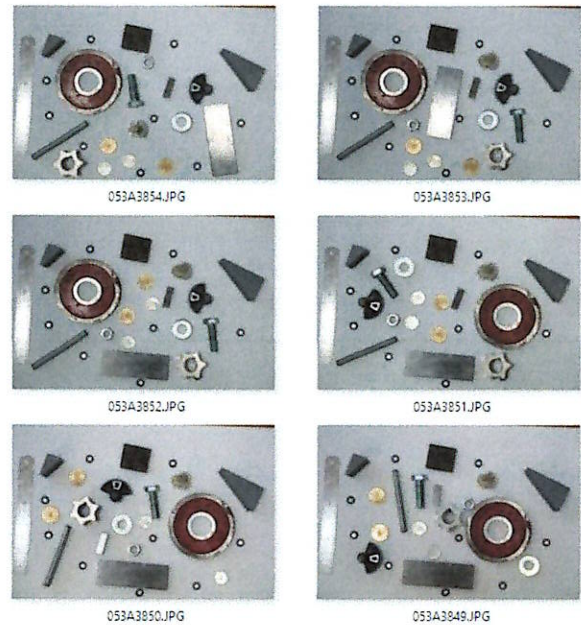


Fig. 3 The images used to validate the mathematical model

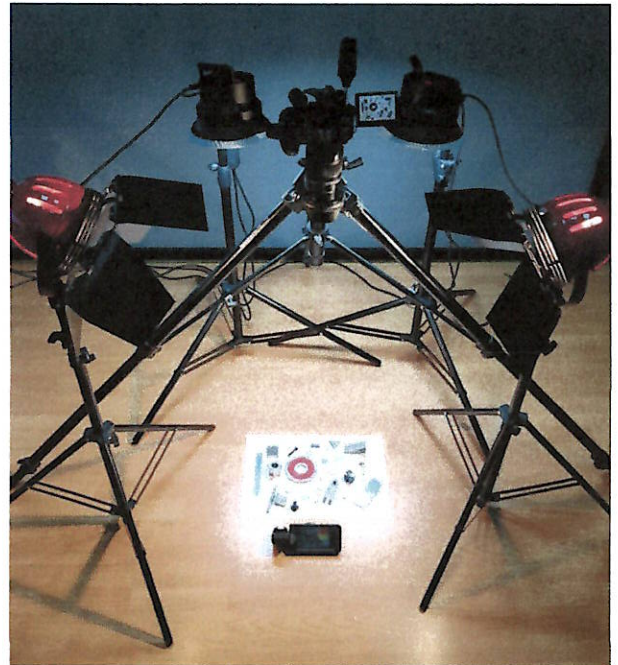


Fig. 4 Image acquisition

The images were acquired using a DSLR Canon 5DSR camera with 50 MPx resolution, the light intensity was measured using Sekonic Spectromaster C-700.

Rozas

3.2. Algorithm automation

The automation of the algorithm was realized using Matlab software. Every image that will be verified will receive an element that will be compared to that image (e.g. coin element for a standard image, or ear element for a work of art). Two regions will be identified, one in the image that is used for comparison and one in the element. For those regions the normalized cross – correlation algorithm will be applied and it will generate an array where these sub regions intersect themselves. This array can later be used in order to identify the position of the element inside the image that was analyzed (e.g. the presence of a coin 2 times in the image, fig.2, or the presence of an ear in a painting, fig.6). The algorithm was tested on three types of images (Fig. 5), one in the visible specter and the other two in the IR and UV specters.

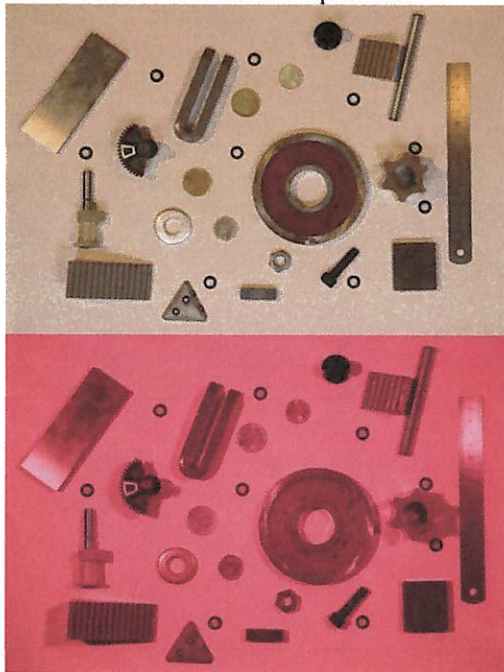





Fig. 5 Types of photos used: visible, IR, UV


The algorithm was successful in identifying the elements in all three types of images that were used, but at different rates and processing time and power. It also showed that using different resolution for the elements modified the processing time and power of the algorithm. The chapter below will present these results.

4. RESULTS

The table below presents a couple of pictures of some of the elements in the paper at different resolutions in order to identify a connection between the resolution and the time required for image processing. The pictures of the elements will be presented at different resolutions.

Table 1 Different resolutions and processing time for elements of the images

Element	Resolution	Processing time
	8688x5692 pixels	20 minutes
	4344x2896 pixels	10 minutes
	2172x1488 pixels	3 minutes
	1086x724 pixels	30 seconds
	8688x5692 pixels	20 minutes
	4344x2896 pixels	10 minutes
	2172x1488 pixels	3 minutes
	1086x724 pixels	30 seconds
	8688x5692 pixels	20 minutes
	4344x2896 pixels	10 minutes
	2172x1488 pixels	3 minutes

	1086x724 pixels	30 seconds
	8688x5692 pixels	20 minutes
	4344x2896 pixels	10 minutes
	2172x1488 pixels	3 minutes
	1086x724 pixels	30 seconds

5. CONCLUSION AND FUTURE WORK

The algorithm was successfully applied on the images that showcased various engineering elements (gauges, screws, washers, coins) as well as the images showcasing the field of cultural heritage. Fig. 6 illustrates the results obtained after the application of the algorithm on a work of art, where the element of interest, (the ear) can be identified in the image.

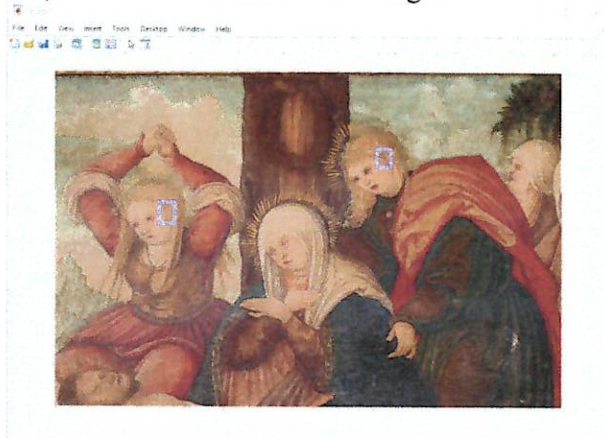


Fig. 6 Results of application of algorithm on art

Time is a factor in image processing. In order to reduce the time needed to process a certain image a series of operations should be performed, such as: reducing the image resolution, choosing an optimal color spectrum for the image.

The algorithm can be successfully applied in the field of cultural heritage, as shown in the example showcased above.

6. ACKNOWLEDGMENTS

The work presented in this paper is supported by a grant of the Romanian Ministry of Research

and Innovation, CCCDI - UEFISCDI, project number PN-III-P1-1.2-PCCDI-2017-0812/53PC CDI, within PNCDI III.

7. REFERENCES

- [1] T. Hurtut, "2D artistic images analysis, a content-based survey", 2010, Available: <https://hal.archives-ouvertes.fr/hal-00459401v1>.
- [2] C. Guccio, M. F. Martorana, I. Mazza, I. Rizzo, "Technology and public access to cultural heritage: the Italian experience on ICT for public historical archives", In *Cultural heritage in a changing world*, pp. 55-75, Springer, 2016.
- [3] V. Petras, T. Hill, J. Stiller, Gäde M., "Europeana – a Search Engine for Digitized Cultural Heritage Material", *Datenbank-Spektrum*, Vol. 17, Iss. 1, pp. 41-46, 2017.
- [4] S. Zhao, et. al., "Exploring Principles-of-Art Features for Image Emotion Recognition", *Proceedings of the 22nd ACM international conference on Multimedia*, pp. 47-56, 2014.
- [5] B. Yaniv, L. Noga, W. Lior, "Classification of Artistic Styles Using Binarized Features Derived from a Deep Neural Network", *Computer Vision - ECCV 2014 Workshops* pp 71-84, 2014.
- [6] H. M. El-Bakry, Zhao Q., "Fast Pattern Detection Using Normalized Neural Networks and Cross-Correlation in the Frequency Domain", *Journal on Applied Signal Processing*, pp. 2054-2060, 2005.
- [7] D. Popescu, et al., "Using image processing to authenticate artwork", *Acta Tehnica Napocensis, Series: Applied Mathematics, Mechanics, and Engineering*, Vol. 61, Iss. 3, pp. 507-511, 2018.
- [8] R. Manduchi, A. M. Gian, "Accuracy analysis for correlation-based image registration algorithms", *IEEE International Symposium on Circuits and Systems*, pp. 834-837, 1993.
- [9] K. Briechle, U. D. Hanebeck, "Template matching using fast normalized cross correlation", *Optical Pattern Recognition XII*, Vol. 4387, pp. 95-102, 2001.
- [10] L. Di Stefano, S. Mattocchia, M. Mola, "An Efficient Algorithm for Exhaustive

- Template Matching based on Normalized Cross Correlation”, Proceedings of the 12th International Conference on Image Analysis and Processing (ICIAP’03), pp. 322-327, 2003.
- [11] J.-C. Yoo, T. H. Han, “Fast normalized cross-correlation”, Circuits, systems and signal processing Vol. 28, Iss. 6, pp. 819-826, 2009.
- [12] R. O. Duda, P. E. Hart, “Pattern Classification and Scene Analysis”, New York: Wiley, 1973.
- [13] R. C. Gonzalez, R. E. Woods, “Digital Image Processing” (third edition), Reading, Massachusetts: Addison-Wesley, 1992.
- [14] J. P. Lewis, “Fast Normalized Cross – Correlation,” Industrial Light & Magic
- [15] D. I. Barnea, H. F. Silverman, “A class of algorithms for fast digital image registration”, IEEE Trans. Computers, Vol. 21, pp. 179-186, 1972.
- [16] J. P. Lewis, “Fast Template Matching”, Vision Interface, pp. 120-123, 1995.

UTILIZAREA PROCESARII IMAGINILOR PENTRU VERIFICAREA AUTENTIFICITATII ARTISTICE

Rezumat: Abordarea tradițională utilizată pentru studiile de artă pictată se bazează pe observațiile studenților privind diferențele subtile în detaliu și caracteristicile de periere. Având în vedere metodele empirice implicate, în unele cazuri interpretarea poate fi influențată de o serie de aspecte, cum ar fi experiența personală, acuitatea vizuală sau percepția individuală a culorilor. Dezavantajele acestei tehnici sunt agravate de lipsa personalului calificat suficient. Lucrarea descrie pașii preliminari necesari dezvoltării platformei "ID-Art", o soluție integrată cu scopul de a furniza cunoștințe științifice complementare și argumente matematice necesare investigării artefactelor 2D sau a altor eforturi de autentificare a operelor de artă pictate.

Rareș GHINEA, Department of Design Engineering and Robotics, Technical University of Cluj-Napoca, Romania, rares.ghinea@muri.utcluj.ro

Vasile TOMPA, Department of Design Engineering and Robotics, Technical University of Cluj-Napoca, Romania, vasile.tompa@muri.utcluj.ro

Zsolt BUNA, Department of Design Engineering and Robotics, Technical University of Cluj-Napoca, Romania, zsolt.buna@muri.utcluj.ro

Raul ROZSOS, Department of Design Engineering and Robotics, Technical University of Cluj-Napoca, Romania, raul.rozsos@muri.utcluj.ro

Daniela POPESCU, Department of Design Engineering and Robotics, Technical University of Cluj-Napoca, Romania, daniela.popescu@muri.utcluj.ro

Ciprian FIREA, The Romanian Academy, Institute of Archaeology and Art History, Cluj-Napoca, Romania, cfirea@yahoo.com